# Study on development of brown and beige adipocytes in mice: effect of age and diet-induced obesity

**(マウスにおける褐色およびベージュ脂肪細胞の誘導・発達に関する研究：加齢および食餌誘導性肥満の影響)**

**Woongchul SHIN**

## AUTHOR'S DECLARATION

This study is my original work and has not been presented at any other University for the award of a degree. A part of this thesis has been published as follow:

Shin WC, Okamatsu-Ogura Y, Machida K, Tsubota A, Nio-Kobayashi J, Kimura K. Impaired adrenergic agonist-dependent beige adipocyte induction in aged mice. Obesity 25:417-423, 2017

**CONTENTS**

## LIST OF TABLES

## LIST OF FIGURES

## ABBREVIATIONS

| | |
|---|---|
| β-AR | β-adrenergic receptor |
| BAT | Brown adipose tissue |
| CL | CL316,243 |
| COX IV | Cytochrome c oxidase subunit IV |
| FDA | Food and drug administration |
| FGF | Fibroblast growth factor |
| HFD | High-fat diet |
| IL-1β/-6 | Interleukin-1β/-6 |
| MCP-1 | Monocyte chemotactic protein-1 |
| JAK | Janus-activated kinase |
| Myf5 | Myogenic factor 5 |
| NE | Norepinephrine |
| ND | Normal diet |
| PDGF | Platelet-derived growth factor |
| PDGFRα/β | Platelet-derived growth factor receptor α/β |
| PET-CT | Positron emission tomography-computed tomography |
| PGC1α | Peroxisome proliferator-activated receptor γ coactivator α |
| PI3K | Phosphatidylinositol 3-kinase |
| PKA | Protein kinase A |
| PPARα/γ | Peroxisome proliferator-activated receptor α/γ |
| PRDM16 | PR domain containing 16 |
| SMA | Smooth muscle actin |
| STAT | Signal transducer-activated transcription |
| SV | Stromal vascular |
| TNFα | Tumor necrosis factor α |
| UCP1 | Uncoupling protein 1 |
| WAT | White adipose tissue |
| WNT | Wingless/intergrated |
| WHO | World health organization |

## PREFACE

Obesity, defined as abnormal or excessive body fat accumulation that may cause an adverse metabolic disorder, is a growing global problem (1). With changing eating habit and life style, obesity prevalence has greatly increased worldwide in the last several decades (2). According to World Health Organization (WHO) reports, more than 1.9 billion adults older than 18 years were overweight or obese in 2016, and obesity has nearly tripled since 1975 (3). It was estimated that at least 2.8 million people die each year as a result of being overweight or obese (4).

Obesity has been recognized as the major risk factor for the development of a number of chronic metabolic disorders, including diabetes, hypertension, cardiovascular diseases and cancer (5, 6). That is, increased accumulation of body fat, especially in visceral area, causes systemic and chronic low-grade inflammation that contributes to the onset of the metabolic disorders (7). At molecular levels, as a consequence of the expansion of adipose tissue, cellular stress such as endoplasmic reticulum stress, mitochondrial dysfunction, and hypoxia causes abnormal production of adipokines, fatty acids, and pro-inflammatory cytokines such as tumor necrosis factor α (TNFα) and interleukin (IL)-6 (8, 9). Hypertrophied adipocytes also secret monocyte chemotactic protein-1 (MCP-1) that recruits macrophages into adipose tissue (8, 10). Infiltrated macrophages are activated by adipocyte-derived fatty acids, and secrete pro-inflammatory cytokine such as TNFα and IL-1ß (8, 11). Chronic exposure of such pro-inflammatory cytokines from macrophages and also adipocytes stimulates their respective cytokine signaling pathways which interfere insulin signaling pathway, thereby leading to insulin resistance (8, 11). Insulin resistance in peripheral tissue and also in endothelial cells causes hyperglycemia, dyslipidemia, and related metabolic diseases (12, 13).

Generally, obesity develops when energy intake chronically exceeds total energy expenditure (14). Thus, strategy for preventing obesity or reducing body fat is increasing

physical activity or reducing calorie intake. In addition, anti-obesity drugs targeting the regulation of appetite or intestinal fat absorption has been approved by the Food and Drug Administration (FDA) and are available in the market in the United States (14). Among them, only the mazindol, an appetite suppressor, is approved in Japan for short-term treatment of individuals with morbid obesity (15). However, these drugs often elicit serious side effects, including anxiety, depression, and steatorrhea. Thus, much safer alternative strategies to treat obesity are needed.

White adipose tissue (WAT) is highly specialized for energy storage. On the other hand, brown adipose tissue (BAT) is the tissue specialized for a non-shivering thermogenesis that dissipates energy as heat. Therefore, BAT attracts a great attention as a therapeutic target of obesity and related metabolic diseases (16, 17). Indeed, BAT consumes lipid and glucose as energy substrates (18, 19). BAT thermogenesis is principally dependent on the activation of mitochondrial uncoupling protein 1 (UCP1), which uncouples oxidative phosphorylation from electron transport system by dissipating energy formed by the electrochemical gradient as heat (20). Activity of UCP1 is mainly controlled by the sympathetic nervous system: norepinephrine (NE) released from nerve endings activates the β-adrenergic receptor (β-AR) on brown adipocytes, resulting in the sequential activation of enzymes including adenylate cyclase, protein kinase A (PKA), hormone-sensitive and adipose triglyceride lipase, and followed by lipolysis (17). Liberated fatty acids activate UCP1 and are simultaneously used as substrates for β-oxydation to form the electrochemical gradient for thermogenesis. Prolonged activation of the β-AR pathway induces hyperplasia of BAT accompanied with elevated UCP1 expression level (18). The role of BAT in the energy expenditure and body fat control has been established in rodents. Activation of BAT by the injection of agonist for ß3-AR increases whole body energy expenditure (19, 21). Chronic treatment with ß3-agonist or intake of some thermogenic compounds results in the BAT hyperplasia and the reduction of adiposity (21-23). In addition,

*Ucp1*-null mice exhibit an obese phenotype when kept in thermoneutral conditions (24). Furthermore, functional thermogenic activity of BAT was proved in adult human, and its amount significantly and negatively correlates with adiposity, suggesting that BAT contributes to body fat control in humans (25, 26). These data indicate that BAT and UCP1 can be an effective target for anti-obesity treatment both in animals and humans.

There is another UCP1-expressing cell, referred to as "beige/brite adipocytes," that appears in WAT after chronic sympathetic stimulation, such as cold exposure (16-18). Beige adipocyte has a thermogenic function like BAT at least *in vitro* (27, 28), but characteristics of its gene expression and cell lineage are quite different from those of brown adipocyte (29-31). Interestingly, characteristics of gene expression in human BAT more closely resembles that of mouse beige adipocyte than brown adipocyte (30, 32). It is accepted that sympathetic nervous system-mediated activation of β3-AR is the most physiologically important pathway for the beige adipocyte induction, because of the following evidence: continuous injection of β3-AR agonist mimics the effect of cold exposure (33, 34), and surgical denervation of sympathetic nerves to inguinal WAT or knockout of β3-AR in mice results in attenuated cold-induced beige adipocyte induction (35, 36). In addition, it is suggested that immune cells and secreted factors such as fibroblast growth factor (FGF) 21 and both atrial and brain natriuretic peptides are involved in the beige adipocyte induction (37-39). However, mechanism(s) to control beige adipocyte induction is not fully understood.

It is well described that visible BAT disappear in young aged middle and large sized animals including human, while BAT is present even in elder aged small animal such as mouse (16-18). Interestingly, recent findings indicate that functional positron emission tomography-computed tomography (PET-CT)-detectable BAT is almost present in young aged lean subjects and almost absent in elder aged subjects (40). In addition, PET-CT-detectable BAT is hard to detect in young aged subject (41). As gene expression profile of human BAT is largely

overlapped with that of mouse beige cells, but not brown adipocytes, I hypothesized the induction of beige adipocyte is depend on age and adiposity.

Thus, the specific aims of the thesis were to:

1. Investigate aging-related changes of brown and beige adipocyte development in mice
2. Investigate obesity-related changes of brown and beige adipocyte development in mice

# CHAPTER 1

# Investigation of aging-related changes of brown and beige adipocyte development in mice

**Introduction**

There are three types of adipocyte in mammals: brown, white and beige adipocytes. White adipocyte stores energy as triglyceride and releases as fatty acids into circulation. In contrast, brown adipocyte uses fatty acids as substrate for β−oxydation as well as activation of UCP1, thereby thermogenesis (14-16). Beige adipocyte is inducible type of UCP1-expressing adipocyte that appears in WAT upon specific stimuli (17-19). It is well accepted that adrenergic signaling pathway is a primary and dominant signal to induce beige adipocyte (14). In addition, macrophages are also suggested to have an important and opposite role in the induction of beige adipocytes. Anti-inflammatory resident M2 macrophages are reported to induce beige adipocytes by synthesizing norepinephrine (NE) in response to cold stimulation (42, 43). On the other hand, pro-inflammatory M1 macrophages migrated into obese state WAT suppress beige adipocyte induction in response to cold stimulation (44).

Although beige adipocytes resemble brown adipocyte in terms of morphology and thermogenic function, they developmentally originate from a myogenic factor 5 (MYF5)-negative lineage which also produce white adipocyte, but not brown adipocyte (20). In addition, it is suggested that beige adipocytes arise through the direct trans-differentiation of pre-existing white adipocytes in response to chronic cold exposure (45, 46). Once the stimulation was removed, beige adipocytes are converted into unilocular white adipocytes accompanied by mitochondria degradation process through mitophagy (47, 48). On the other hand, Wang et al. used AdiopoChaser mice to label mature adipocyte *in vivo,* and showed that most of the beige adipocytes induced by cold exposure in the subcutaneous WAT are derived from a precursor population rather than from mature white adipocytes (49). It was also reported that stromal cell expressing platelet-derived growth factor receptor α (PDGFRα) can differentiate into both beige and white adipocytes, in response to cold exposure and high-fat diet feeding, respectively. Isolated PDGFRα-expressing cell were shown to differentiate into UCP1-expressing adipocyte

by β3-adrenergic stimulation *in vivo* (50). These results suggest that PDGFRα-positive cell in WAT is progenitor of both beige and white adipocyte. However, it is not known that single PDGFRα-positive progenitor in WAT contributes to beige adipocyte development in size.

It is well established that in large mammals, the amount of BAT decreases with growth and is hardly detectable in adults with reduced UCP1 expression (16). Small rodents, such as mice and rats, possess a significant amount of BAT throughout their life, but the function of BAT is reported to decrease with aging (51-53). It is shown that cell proliferation and UCP1 expression are low in BAT of aged rats compared to young rat (54). In humans, the prevalence of functional BAT decline with aging (55-57), suggesting that beige adipocyte is also affected by aging. However, there is little information on aging-related change in beige adipocyte induction. In this chapter, I investigated aging-dependent changes of brown and beige adipocytes in mice in response to ß3-adrenergic stimulation.

## Methods

### *Animals and tissue sampling*

The experimental procedures and care of animals were approved by the Animal Care and Use Committee of Hokkaido University (Approved number: 09-0039). All experiments using mice were conducted in the animal facility approved by the Association for Assessment and Acheeditation of Laboratory Animal Care (AAALAC) International. Male 4-month-old and 20-month-old C57BL/6J mice were housed in plastic cages placed in an air-conditioned room at 23 °C with a 12:12h light: dark cycle and given free access to laboratory chow (Oriental Yeast, Tokyo, Japan). The mice were daily subcutaneously injected with β3-adrenergic receptor agonist CL316,243 (CL; 0.1 mg/kg, once a day; American Cyanamid, Pearl River, NY, USA) or saline, as a control, for 1 week. Then mice were euthanized with carbon dioxide, and interscapular BAT, inguinal WAT, and perigonadal WAT were quickly removed and transferred into liquid nitrogen for western blot analysis, RNAlater storage solution (Ambion, Austin, TX, USA) for quantitative PCR analysis, 10% phosphate-buffered formalin for histological examination, or used for the isolation of stromal-vascular (SV) fraction and flow cytometry analysis.

### *Isolation of the stromal vascular (SV) fraction*

Adipose tissue fragments were cut into small pieces and incubated in DMEM containing 2% fatty acid-free bovine serum albumin (Sigma-Aldrich Fine Chemical, St Louis, MO, USA) and 2 mg/ml collagenase (Wako Pure Chemical Industries, Osaka, Japan) at 37 °C for 2 h with shaking at 100 cycles/min. The suspension was filtered through a 200 μm nylon filter and centrifuged at 120 × g for 5 min at room temperature. The pellet was suspended in ACK erythrocyte lysis buffer (150 μM $NH_4Cl$, 10 mM $KHCO_3$, 1 mM EDTA-2Na). The sample was centrifuged at 120 × g for 5 min at room temperature. The pellet was suspended in PBS

containing 2% fetal calf serum (FCS) and used for flow cytometry analysis.

***Flow cytometry analysis***

The SV fraction was incubated with a mixture of antibodies containing either anti-CD31-PE-Cy (BioLegend, San Diego, CA, USA), anti-CD34-PE (BioLegend), anti-Sca1-PerCP/Cy5.5 (BioLegend), and anti-PDGFRα (CD140a)-APC (BioLegend) or containing anti-CD11c-FITC (BD bioscience, San Jose, CA, USA), anti-CD206−PerCP/Cy5.5 (BioLegend), and anti-F4/80-APC (BioLegend) for 30 min on ice. After centrifugated at 1,000 × g for 10 min at 4 °C, the supernatant was discarded and the pellet was suspended in PBS containing 2% FCS. The suspension was filtered through a 40 μm nylon filter and analyzed on a flow cytometer (BD FACSVerse, BD biosciences) with singlet discrimination to detect APC, PE-Cy, PE, and PerCP/Cy5.5 stained cells.

***mRNA analysis***

Total RNA was extracted using the RNAiso reagent (Takara Bio, Shiga, Japan) according to the manufacturer's protocol. Total RNA (2 μg) was treated with DNAase I (Roche Diagnostics, Mannheim, Germany) and reverse transcribed using a 15-mer oligo(dT) adaptor primer and M-MLV reverse transcriptase (Promega, Madison, WI, USA). Real-time PCR was performed on a fluorescence thermal cycler (LightCycler system; Roche) using FastStart Essential DNA Green Master (Roche). Absolute expression levels were determined using a standard curve method, with respective cDNA fragments as standards. The mRNA levels are expressed as relative values compared to β-actin mRNA levels. The primers used in this study are listed in Table 1.

***Protein analysis***

Tissue specimens were homogenized in Tris-EDTA buffer (10 mM Tris and 1 mM EDTA, pH 7.4). The sample was centrifuged at 800 × *g* for 10 min at 4 °C, and the fat-free supernatant was then collected and used for protein concentration measurement and western blot analysis. For western blot analysis, proteins were separated by SDS-PAGE and transferred to a polyvinylidene fluoride membrane (Immobilon; Millipore, Tokyo, Japan). After blocking the membrane with 5% skim milk (Morinaga Milk Industry Co., Tokyo, Japan), it was incubated with a primary anti-rat UCP1 antibody, a kind gift from Prof. Teruo Kawada (Kyoto university), with an anti-bovine cytochrome oxidase complex 4 antibody (COX4; Molecular Probes, Eugene, OR, USA), or with an anti-ß-actin antibody (Sigma) for 1 h. The bound antibody was visualized using horseradish peroxidase-linked goat anti-rabbit immunoglobulin (Cell Signaling Technology, Danvers, MA, USA) for the detection of UCP1 or horseradish peroxidase-linked goat anti-mouse immunoglobulin (Cell Signaling Technology) for the detection of COX4 and an enhanced chemiluminescence system (Millipore). Total UCP1 or COX4 content (arbitrary unit per depot) was calculated by multiplying the protein amount detected by western blot (arbitrary unit per μg protein) by the total protein amount extracted from the whole depot (μg per depot).

***Histology***

Tissue specimens fixed in 10% formalin were embedded in paraffin, cut into 4-μm-thick sections, and the sections were stained with hematoxylin and eosin. The stained samples were examined under a light microscope.

***Data analysis***

Values are expressed as means ± SE. Statistical analysis was performed using Student's *t*-test or ANOVA followed by Tukey's post-hoc test. All these statistical analyses were

performed using SPSS software.

**Results**

The body weight of aged mice (age 20 months) was higher than that of young mice (age 4 months) (Young, 28.0 ± 1.5 g; Aged, 33.1 ± 1.4 g). This was accompanied by an increase in BAT and perigonadal WAT (gWAT) weight (Figure 1-1). The brown adipocytes of aged mice had larger lipid droplets in the cytoplasm (Figure 1-2) and the size of white adipocytes also larger than those of young mice (Figure 1-2), indicating age-related accumulation of body fat.

Young mice that received ß3-AR agonist, CL316,243 (CL)-injection for 1 week showed no obvious decrease in body weight (27.2 ± 1.8 g) or adipose tissue weight (Figure 1-1), but demonstrated decreased brown and white adipocyte size, resulting in a dense appearance of the tissue as compared to the saline-injected young mice (Figure 1-2). In addition, multilocular adipocytes similar morphology to brown adipocytes in the BAT, appeared in the inguinal WAT (iWAT), suggesting induction of beige adipocytes upon β3-adrenergic stimulation (Figure 1-2). The body (32.2 ± 0.9 g) and adipose tissue weight (Figure 1-1) of aged mice that received CL-injections also did not alter compared to saline-injected aged mice but exhibited decreased adipocyte size in all depots. However, the appearance of multilocular adipocytes in the iWAT was reduced in aged mice compared with young mice.

To quantify the numbers of beige adipocytes in the iWAT, expression of uncoupling protein 1 (UCP1) was examined. Saline-injected aged mice expressed comparable amount of UCP1 in BAT to that of saline-injected young mice, whereas both groups of mice showed no UCP1 expression in the iWAT (Figure 1-3A). CL-injection enhanced the UCP1 expression in the BAT of both aged and young mice (Figure 1-3A). In addition, CL-injected young mice showed a statistically significant increase in UCP1 expression in iWAT as compared to saline-injected mice (Figure 1-3B). While CL-injected aged mice had detectable UCP1 by western blot, the increase was not statistically significant as compared with saline-injected aged mice (Figure 1-3B). The analysis of another mitochondrial protein, cytochrome c oxidase 4 (COX4),

in BAT and iWAT showed similar trends (Figure 1-3). Taken together, these results indicate impaired β3-adrenergic agonist-mediated induction of beige adipocytes in iWAT from aged mice.

To determine the underlying mechanisms by which β3-adrenergic agonist-mediated induction of beige adipocytes was impaired in iWAT from aged mice, change in mRNA expressions of ß1- and ß3-AR was examined. Inconsistent with the previous report (58), there were no significant differences in expression of the receptors between young and aged mice, irrespective of CL treatment (Figure 1-4A). In addition, expression of macrophage markers, F4/80 and tumor necrosis factor α (TNFα), were also examined, as adipose tissue from obese animal shows an increase in the number of infiltrating inflammatory M1 macrophages (59). Again, there was no significant difference in the expression of either marker in iWAT among the four groups (Figure 1-4B). Consistent with this, analysis of the cellular population in the stromal vascular (SV) fraction from iWAT by flow cytometry showed no difference in M1 or M2 macrophage populations between the young and aged mice (Figures 1-5D).

Macrophages comprised only 5.8% of SV cells from iWAT in young mice (Figure 1-5D). Endothelial cells and PDGFRα-expressing cells, reported to be progenitors for beige adipocytes (50), accounted for 12% and 39.3% of SV cells, respectively, in this group. It is worth to note that aged mice possessed a smaller number of PDGFRα-expressing cells in iWAT (27.1% ± 4.3%) than young mice (39.3% ± 2.4%), although there was no statistically significant difference in the endothelial cell population between aged and young mice (Figure 1-5 D). In BAT, endothelial cells and PDGFRα-expressing cells accounted for 38.1% and 18.3% of SV cells, respectively (Figure 1-5 C), and there was no difference in these cell populations between young and aged mice.

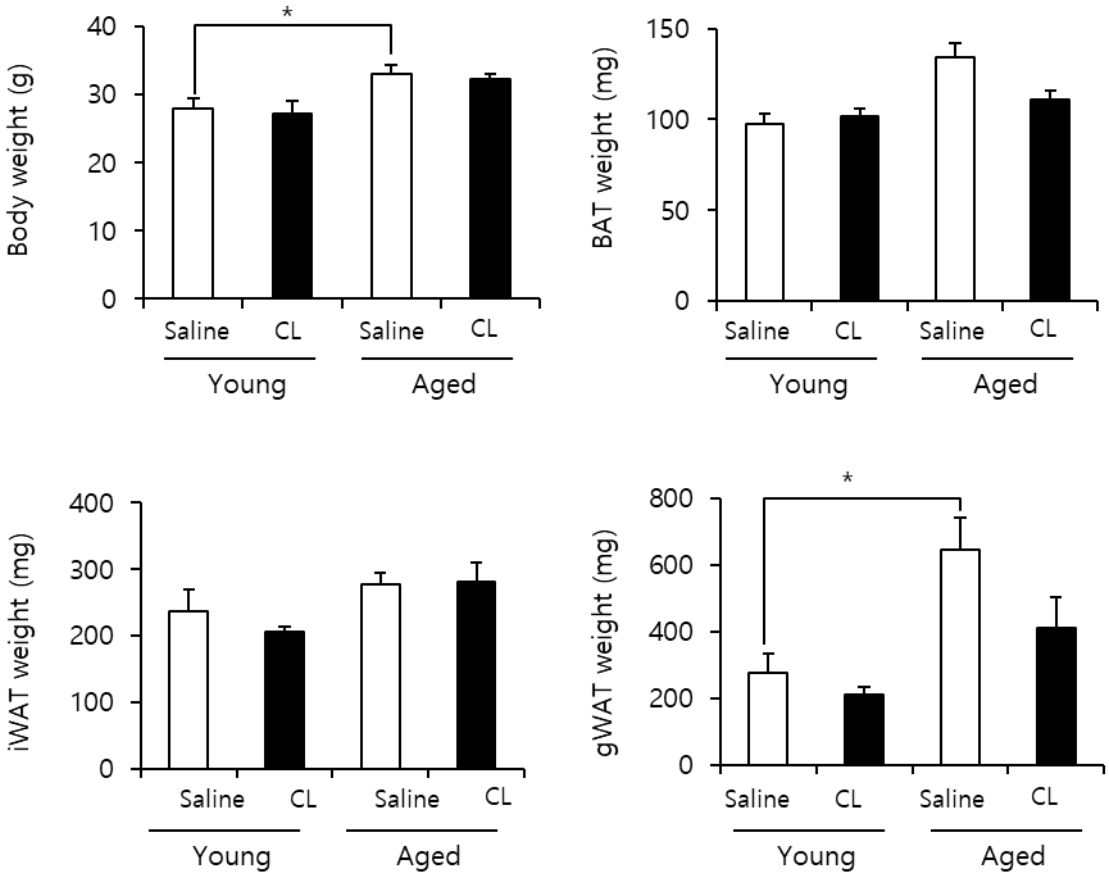


**Figure 1-1 Effect of $\beta$3-adrenergic agonist on the weight of adipose tissue in young and aged mice**

(A) Young (age 4 months) and aged (age 20 months) C57BL/6J mice received daily injections of saline or CL316,243 (CL; 0.1 mg/kg, sc, once a day) for one week. Body weight was measured. Interscapular brown adipose tissue (BAT) and inguinal (iWAT) and perigonadal (gWAT) white adipose tissues were excised and their weights were measured. Values are expressed as means ± SE for 3–4 mice. *p < 0.05 by ANOVA.

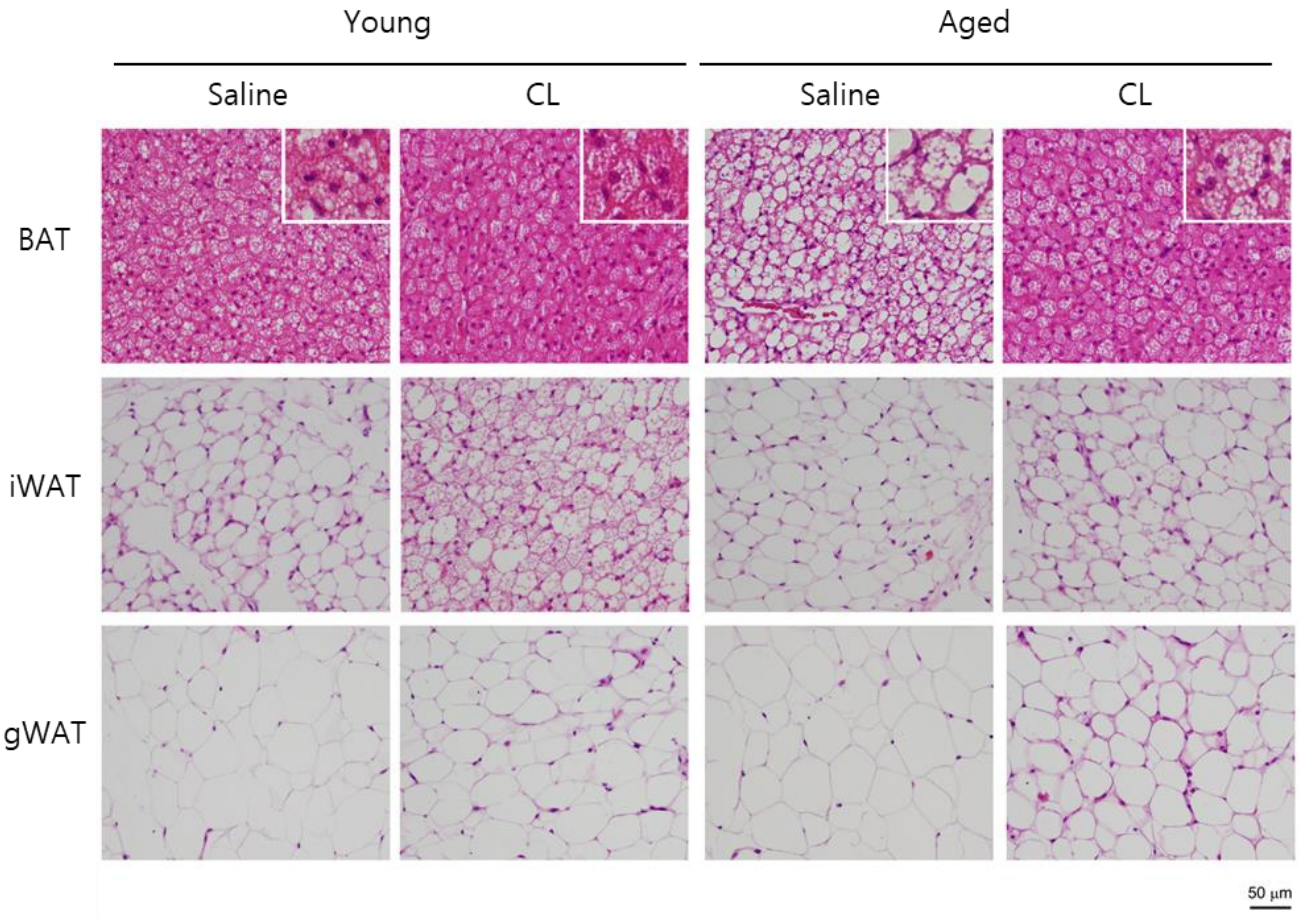


**Figure 1-2 Effect of $\beta$3-adrenergic agonist on morphological features of adipose tissue in young and aged mice**

Representative images of the sections stained with hematoxylin and eosin of BAT, iWAT, and gWAT of saline or CL-injected young and aged mice. The inserts show enlarged image of the sections.

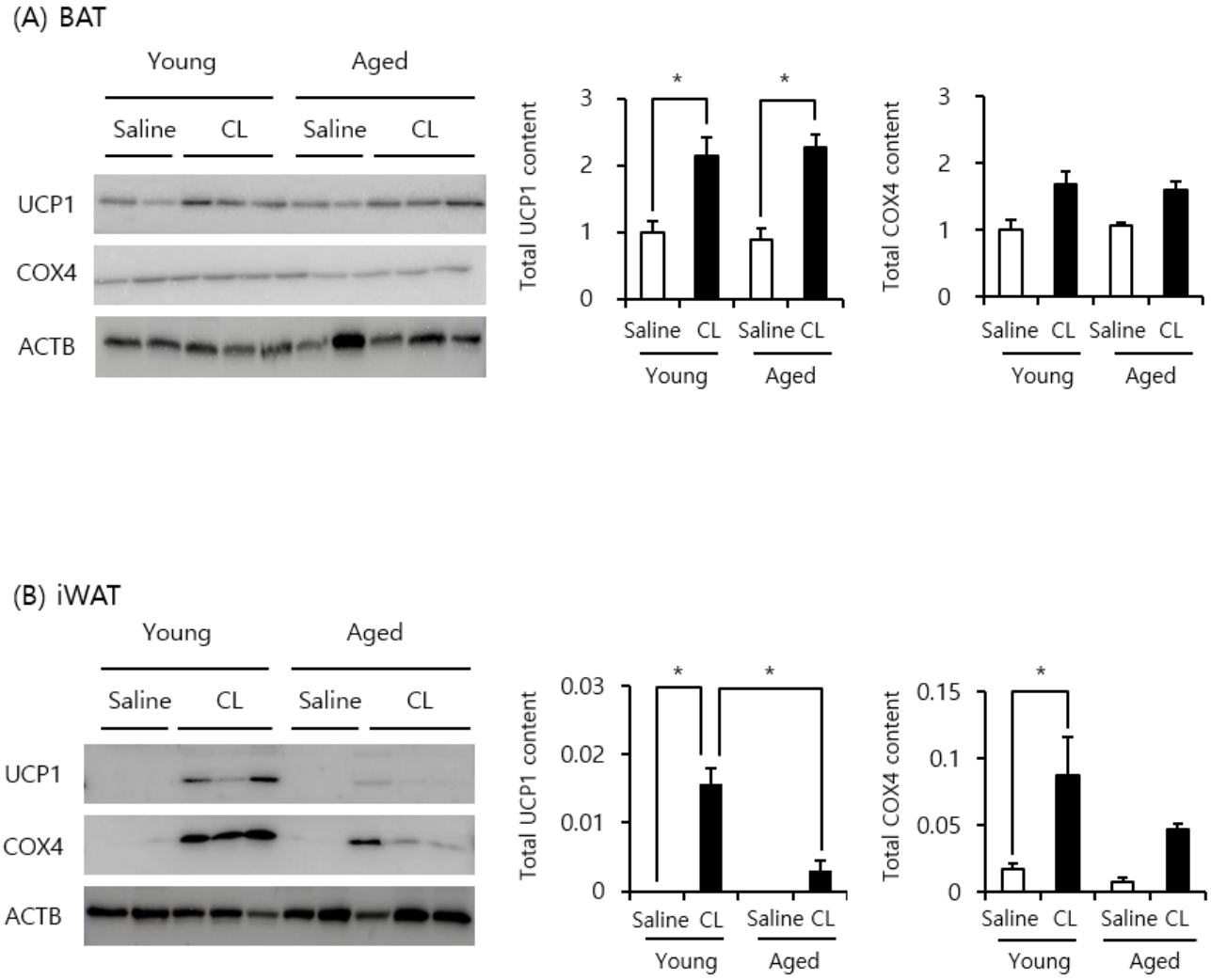


**Figure 1-3 Effect of $\beta$3-adrenergic agonist on protein expression in the adipose tissues of young and aged mice**

UCP1 and COX4 protein levels in BAT (A) and iWAT (B) of saline- or CL-injected young and aged mice were analyzed by western blotting using 2.5 μg and 10 μg of total protein extracted from BAT and iWAT, respectively. ACTB is shown as a loading control. Total content of UCP1 and COX4 per depot was estimated by multiplying the protein amount detected by western blotting (arbitrary unit per μg protein) by the total protein extracted from whole depot (μg per depot), and expressed as relative value to the respective amounts in BAT of saline-injected young mice. Values are expressed as means ± SE for 3–4 mice. *p < 0.05 by ANOVA.

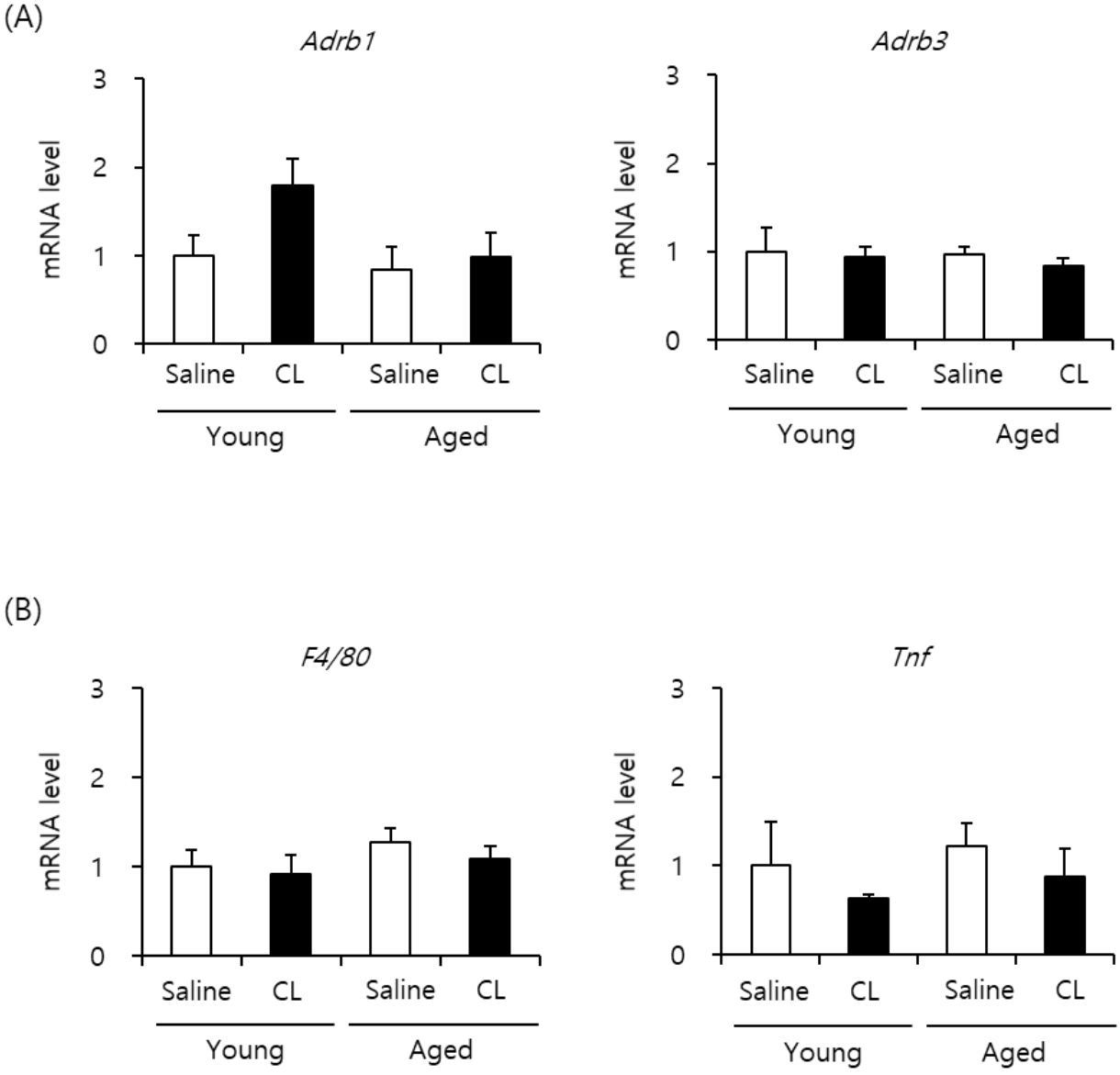


**Figure 1-4 Effect of β3-adrenergic agonist on mRNA expressions in inguinal white adipose tissue of young and aged mice**

Expression of the genes in iWAT of saline- and CL-injected young and aged mice was analyzed by quantitative real-time PCR. Expression of $\beta$1- and $\beta$3-adrenergic receptor (Adrb1 and Adrb3) (A) and macrophage marker F4/80, and *Tnf* (B) are shown. Data normalized to *Actb* expression are expressed as relative value to saline-injected young mice. Values are expressed as means ± SE for 3–4 mice by ANOVA.

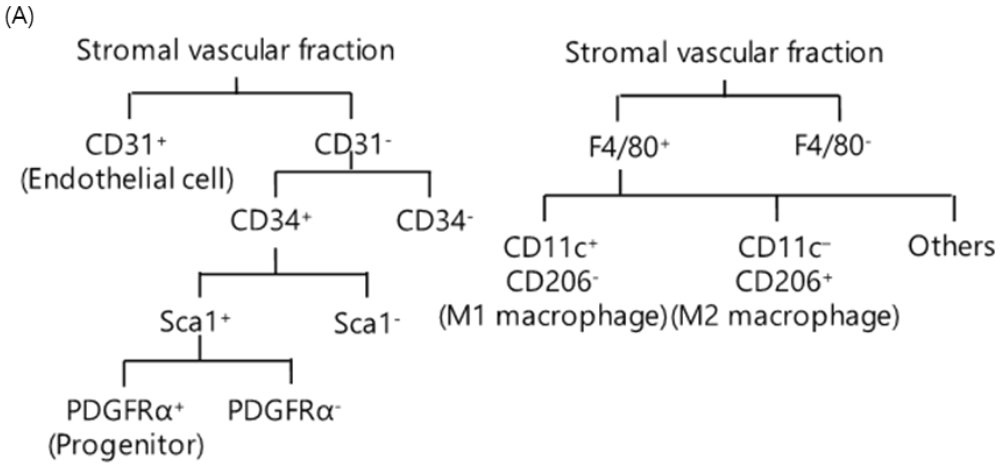
(A)
Stromal vascular fraction
CD31+
(Endothelial cell)
CD31-
CD34+
CD34-
Sca1+
Sca1-
PDGFRα+
(Progenitor)
PDGFRα-
Stromal vascular fraction
F4/80+
F4/80-
CD11c+
CD206-
(M1 macrophage)
CD11c-
CD206+
(M2 macrophage)
Others

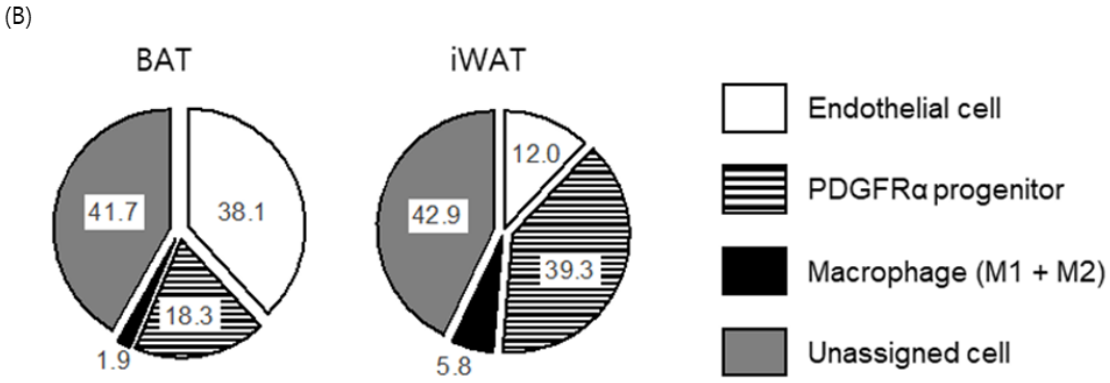
(B)
BAT
iWAT
41.7
38.1
18.3
1.9
42.9
12.0
39.3
5.8
Endothelial cell
PDGFRα progenitor
Macrophage (M1 + M2)
Unassigned cell

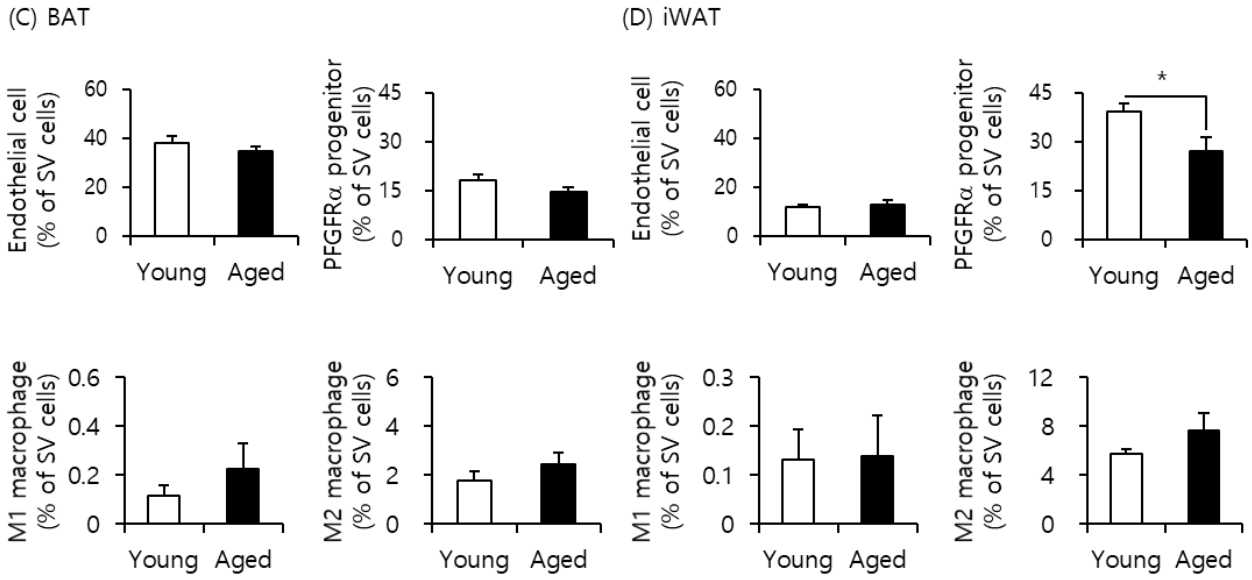
(C) BAT
(D) iWAT
Endothelial cell (% of SV cells)
PFGFRα progenitor (% of SV cells)
M1 macrophage (% of SV cells)
M2 macrophage (% of SV cells)
Young
Aged
*

**Figure 1-5 The number of PDGFR$\alpha$-expressing progenitor in the stromal vascular fraction of brown and inguinal white adipose tissues in young and aged mice**

(A) Diagrams showing a summary of cell surface markers used to separate vascular endothelial cells ($CD31^+$), PDGFR$\alpha$-expressing progenitors ($CD31^-$, $CD34^+$, $Sca1^+$, $PDGFR\alpha^+$), M1 macrophages ($F4/80^+$, $CD11c^+$, $CD206^-$), and M2 macrophages ($F4/80^+$, $CD11c^-$, $CD206^+$) from the stromal vascular (SV) fraction of BAT and iWAT by flow cytometry. (B) Pie graph shows the cellular composition of the SV fraction from BAT and iWAT of young mice. Comparison of cell population in BAT (C) and iWAT (D) between young and aged mice. Values are expressed as means $\pm$ SE for 7 mice. *$p < 0.05$ by Student's *t*-test.

**Discussion**

It is well known that aging leads to a decline in the amount of functional brown adipocytes in large mammals (16). In this study, I observed the lipid droplet size in the BAT of aged mice was much larger than that in young mice, suggesting a lowered BAT activity. However, UCP1 protein content in the BAT was not different between young and aged mice. In contrast to our results, it has been reported that *Ucp1* mRNA expression in BAT decreases with aging (51). The reason for this discrepancy is not clear, but mRNA and protein amounts of UCP1 might not always show direct correlation because of post-translational modification or turnover (60). In addition, mRNA expression is often normalized to housekeeping genes, and hence is largely affected by the cellular composition of each tissue. In fact, aging-associated accumulation of non-adipocyte cells in adipose tissue has been reported (61-63). Therefore, I compared UCP1 content per whole depot to estimate the thermogenic function of the BAT and could not find a difference between young and aged mice, and the BAT of young and aged mice similarly responded to the ß3-AR agonist by increasing UCP1 content. Thus, in this study, no evidence was obtained for the aging-associated decline in function nor BAT response to ß3-AR stimulation in the BAT.

In contrast to the BAT, iWAT showed aging-related decline in the inducibility of beige adipocytes in response to ß3-AR stimulation. Daily injection of ß3-AR agonist for one week induced multilocular beige adipocytes and increased UCP1 protein expression both in young and aged mice in iWAT, but these responses were attenuated in aged mice. Interestingly, it was reported that basal *Ucp1* mRNA expression in subcutaneous WAT, without any inductive stimulation of beige adipocytes, decreases with age in mice (58). In our study, the protein levels of UCP1 in iWAT of saline-injected mice were undetectable by western blot analysis. In addition, previously published report demonstrated that adipocytes isolated from iWAT of non-treated mice do not increase oxygen consumption after NE stimulation (27). Thus, it is unlikely

that basal *Ucp1* mRNA level is an appropriate indicator to estimate the number of the functional beige adipocytes, but it may reflect the inducibility of beige adipocyte. I found no difference in the mRNA expression of ß3-AR between young and aged iWAT. These results are inconsistent with the observation of Rogers et al. that ß3-AR expression decreases with aging (58). The reason for the discrepancy is not clear, however, the possible explanation could be the difference in the age of animals used in the two studies: I used as the young group 16-week-old mice, in which *Ucp1* basal mRNA expression was shown to be already started to decline in the study of Rogers et al. Further study will be needed to clarify how aging affects the expression of ß3-AR.

Recent studies demonstrated that proinflammatory macrophages and cytokines can suppress the induction of UCP1 expression in iWAT in response to the cold exposure (44, 64). In addition, proinflammatory signals increase in visceral WAT with aging (65). Thus, I assumed that the age-dependent decline in beige adipocyte induction may be attributed to the accumulation of macrophages in the iWAT. However, I found no alteration of macrophage number nor changes in the expression of TNFα in the iWAT of aged mice, suggesting that aging-associated changes in beige adipocyte induction are not directly related to macrophage infiltration. Instead, I found that the number of the PDGFRα-expressing progenitors in iWAT significantly decreased in aged mice which was recently demonstrated as progenitor cell for beige adipocyte (50). Thus, it is likely that the aging-dependent decrease in the number of PDGFRα-expressing progenitor may contribute to the attenuation of beige adipocyte induction. On the other hand, the reduction of UCP1 induction in aged mice was more apparent (20% of that in young mice) than that of PDGFRα-expressing progenitor number (70% of that in young mice), suggesting other mechanisms are also involved. It was recently reported that smooth muscle actin (SMA)-expressing mural cells leave their vascular niche to generate UCP1-expressing beige adipocytes in response to cold stimulation (66). Interestingly, cellular

senescence promoted by the overexpression of p21, an inhibitor of cycline-dependent kinase that induce cell-cycle arrest, specifically in SMA-expressing cell significantly suppressed the differentiation of beige adipocyte (66). It was also reported that expression of p53, tumor suppressor that induces cellular senescence, increases in WAT with aging (67). Genetical and pharmacological inhibition of p53 specifically in adipocyte restored ageing-related attenuation of beige adipocyte induction and increased whole-body energy expenditure and insulin sensitivity (67). Thus, aging-dependent cellular senescence especially in progenitor including PDGFRα-cell may also contribute to the age-related decline of beige adipocyte induction.

Human brown fat is a therapeutic target for obesity and related-disease, but the amount of brown fat decreases with aging (40). The mechanisms for this age-dependent decline in human brown fat remain to be elucidated. Interestingly, human adult brown fat resembles the murine beige adipocyte, rather than the brown adipocyte in regarding to gene expression patterns (30, 32). Although there may be species differences, this study may have implication for the age-dependent decline of human brown fat and may propose a new approach to avoid obesity by maintaining appropriate number of beige adipocytes.

**Summary**

In the chapter 1, I investigated the aging-related change of brown and beige adipocyte development in mice. Aged (age 20 months) mice had higher body weight than young (4 month) mice, accompanied with an increase in peri-gonadal WAT weight and enlargement of adipocyte size, which is agree with the well-documented fact of the development of obesity in aged animal. Treatment with CL, an agonist for ß3-AR, increased UCP1 protein amount in both BAT and inguinal WAT, suggesting activation of brown and beige adipocytes. However, induction of beige adipocytes was impaired in aged mice, whereas brown adipocyte activation was comparable to young mice. The number of PDGFRα-expressing progenitor cells, which were reported to differentiate into beige adipocytes, significantly decreased in inguinal WAT of aged mice compared with that of young mice. These results revealed that inductive ability of beige adipocytes in WAT declines with aging in mice. It may be partly because of a decreased number of progenitor cells associated with aging.

Table1: Primer sequences for quantitative real time PCR used in the Chapter 1

| Gene name (gene symbol): NCBI Reference Sequence number, Product size<br>Forward primer sequence<br>Reverse primer sequence |
|---|
| *Actb*: NM_007393.5, 234 bp |
| For: 5’ - TCG TTA CCA CAG GCA TTG TGA T - 3’ |
| Rev: 5’ - TGC TCG AAG TCT AGA GCA AC - 3’ |
| *Adrb1*: NM_007419.2, 169 bp |
| For: 5’ - TTC GCT ACC AGA GTT TGC TG - 3’ |
| Rev: 5’ - GTG ACG AAA TCG CAG CAC TT - 3’ |
| *Adrb3*: NM_013462.3, 130bp |
| For: 5’ - TTC CGT CGT CTT CTG TGT AG - 3’ |
| Rev: 5’ - GCG CAC CTT CAT AGC CAT CA - 3’ |
| *F4/80*: NM_010130.4, 165bp |
| For: 5’ - CTT TGG CTA TGG GCT TCC AGT - 3’ |
| Rev: 5’ - GCA AGG AGG ACA GAG TTT ATC GTG - 3’ |
| *Tnf*: NM_013693.3, 71 bp |
| For: 5’ - ACC CTC ACA CTC AGA TCA TCT TC - 3’ |
| Rev: 5’ - TGG TGG TTT GCT ACG ACG T - 3’ |

# CHAPTER 2

# Investigation of obesity-related changes of brown and beige adipocyte development in mice

**Introduction**

Development of beige adipocytes was attenuated with aging as shown in chapter 1. Aging is closely associated with increased adiposity as the result of the decreased metabolic rate (68). Also, it is well described that accumulated fat is associated with alterations in adipose tissue inducing abnormal expression of adipokines and chronic low-grade inflammation induced by macrophage infiltration (69), which may contribute to the attenuation of beige adipocyte induction. In fact, cold-induced *Ucp1* mRNA expression is downregulated in WAT, accompanied by the increase in the expressions of TNFα, MCP-1 and other inflammation markers, in obese mice (70). In addition, UCP1 expression induced by adrenergic receptor agonist, isoproterenol in C3H10T1/2 adipocytes is suppressed by co-culture with RAW264.7 macrophages (71). Thus, it is reasonable to assume that the impairment of beige adipocyte induction in aged mice is due to the development of age-related obesity.

As shown in chapter 1, the aging-dependent reduction of PDGFRα-expressing progenitor cell number was the most likely mechanism explaining for the ageing-related attenuation of beige adipocyte development. Since PDGFRα-expressing progenitor is reported to have an ability to differentiate into beige adipocyte, it is required to understand the regulatory mechanism of PDGFRα-expressing progenitor induction. Interaction of PDGF dimer as a ligand with its receptor PDGFR regulates the cellular processes of proliferation, migration, and differentiation in cell population of mesenchymal origin. Four different polypeptides generate from four different genes: PDGF-A, PDGF-B, PDGF-C, and PDGF-D (72), and three homodimers, PDGF-AA, PDGF-BB and PDGF-CC, and one heterodimer, PDGF-AB exclusively act through PDGFRα, while PDGF-DD activates PDGFRβ. (72, 73). PDGF binding to the receptor induces the receptor dimerization, sequential activation of receptor tyrosine kinase and autophosphorylation, which in turn activates downstream signal molecules such as phosphatidylinositol 3-kinase-protein kinase B/Akt (PI3K-Akt), Janus-activated

kinase-Signal transducer-activated transcription (JAK-STAT), and phospholipase C (72-74). It is recently reported that PDGF-CC secreted from endothelial cell induces beige adipocyte in WAT, and enhances whole body energy expenditure and improves glucose tolerance in HFD-induced obese mice (75). Thus, it is possible that the change in the expression or action of PDGFs in WAT may affect beige adipocyte induction. Wingless/integrated (WNT) signaling pathway, which regulates proliferation and differentiation of various type of stem cells or progenitors, is also known to affect the PDGF signaling pathway through the enhancement of PDGFRα expression (76, 77). WNT signaling is complex pathway which includes 19 kinds of ligands: WNTs, a large family of cysteine-rich secreted glycoproteins, and 10 kinds of receptors: Frizzled, and numerous transcriptional effectors. Recently, among the several isoforms, WNT10 is reported to be expressed in WAT (77-79), and the inhibition of WNT signaling by C59, a potent inhibitor, enhances the differentiation of preadipocyte into UCP1-expressing cell *in vitro* (80). These results suggest that PDGFs an WNT signaling pathway are possibly involved in the regulation of PDGFRα-expressing progenitors in WAT, however, there is little information on the effect of obesity on these factors in WAT.

In this chapter, I investigated whether the obesity changes the beige adipocyte development and also the number of PDGFRα-expressing progenitors using HFD-induced obese mice. In addition, to understand the mechanism to regulate the number of PDGFRα-expressing progenitors, the involvement of PDGF and WNT signaling was examined.

## Methods

### *Animals, treatment and sampling*

The experimental procedures and care of animals were approved by the Animal Care and Use Committee of Hokkaido University (Approved number: 15-0048, 17-0097). All experiments using mice were conducted in the animal facility approved by the AAALAC. Male C57BL/6J mice were housed in plastic cages placed in an air-conditioned room at 23 °C with a 12:12h light: dark cycle. To examine the effect of obesity, 7-week-old mice were fed with high-fat diet (HFD; D12451, 45kcal % fat, Research diets, New Brunswick, NJ, USA) or control diet (ND; D12450B, 10kcal % fat, Research diets) for 14 weeks. The mice were daily single subcutaneously (s.c.) injected with β3 adrenergic receptor agonist CL316,243 (CL, 0.1 mg/kg) for 1 week before sacrifice.

To examine effect of TNFα, mice were administered intraperitoneally (i.p) with murine TNFα (100 μg/kg/day, Wako pure chemical) or saline for 3 days. At the last TNFα-injection, CL (0.1 mg /kg, s.c.) was also injected.

To examine effect of PDGFR inhibitor, mice were administered with imatinib mesylate (100 mg/kg/day, i.p., Wako pure chemical) or saline for 10 days. From the fourth day of imatinib mesylate-injection, CL (0.1 mg /kg, s.c.) were also injected for 7 days.

After the treatments, mice were euthanized with carbon dioxide, and interscapular BAT and inguinal WAT were quickly removed and transferred into liquid nitrogen for western blot analysis, RNAlater storage solution for quantitative PCR analysis, 10% phosphate-buffered formalin for histological examination, or used for the isolation of stromal-vascular (SV) fraction and flow cytometry analysis.

### *Isolation of the stromal vascular (SV) fraction and flow cytometry analysis*

Isolation of SV fration from iWAT and flow cytometry analysis were conducted as

described in the method of chapter 1.

***mRNA analysis***

The mRNA analysis was performed as described in the method of chapter 1, except RNA without DNase treatment was used. The primers used in this chapter are listed in Table 2.

***Protein analysis***

Isolation of protein from homogenized BAT and iWAT and western botting analysis were conducted as in described in method of chapter 1.

***Histology***

Tissue specimens fixed in 10% formalin were embedded in paraffin, cut into 4-μm-thick sections, and the sections were stained with hematoxylin and eosin. The stained samples were examined under a light microscope.

***Data analysis***

Values are expressed as means ± SE. Statistical analysis was performed using Student's *t*-test or ANOVA followed by Tukey's post-hoc test. All these statistical analyses were performed using SPSS software.

**Results**

To examine the effect of HFD-induced obesity on beige adipocyte induction, mice were fed with normal diet (ND: 10kcal % fat) or high-fat diet (HFD: 45 kcal % fat) for 14 weeks. The final body weight of HFD mice was 36% higher than that of ND mice (ND, 30.6 ± 0.7 g; HFD, 41.5 ± 1.0 g). This was accompanied by an increase in BAT and WAT weight (Figure 2-1). The brown adipocytes of HFD mice had larger lipid droplets in the cytoplasm (Figure 2-2) and the size of white adipocytes also larger than those of ND mice (Figure 2-2), indicating HFD feeding induces obesity with accumulation of body fat. ND mice that received ß3-AR agonist, CL316,243 (CL)-injection for 1 week showed multilocular adipocytes appeared in iWAT, suggesting induction of beige adipocytes upon β3-adrenergic stimulation (Figure 2-2). However, the appearance of multilocular adipocytes in iWAT was significantly reduced in obese mice with HFD, compared with ND mice (Figure 2-2).

To assess the degree of beige adipocytes induction in iWAT, expression of *Ucp1* mRNA was examined. Basal *Ucp1* mRNA expression in BAT from mice fed with HFD was comparable to that of mice fed with ND (Figures 2-3 A). It increased about two-fold after CL-injection, in both mice given ND and HFD. Similar changes in the mRNA expression of cytochrome c oxidase 4 (COX4), a mitochondrial marker, were observed in the BAT of mice fed with either ND or HFD, while there was no alteration in the mRNA expression of peroxisome proliferator-activated receptor gamma coactivator 1-alpha (PGC1α*),* a coactivator for induction of *Ucp1* and *Cox4* genes, and genes related with mitochondria-genesis. *Ucp1* mRNA expression in iWAT from mice fed with ND was enhanced more than 5-fold by CL-injection, accompanied with increased expression of *Cox4* and *Pgc1* mRNA (Figures 2-3 B). However, these gene expression in iWAT from mice fed with HFD failed to respond to CL-injection.

Consistent with the mRNA expression, CL-injection enhanced UCP1 protein levels in the

BAT as well as COX4, suggesting increase in mitochondria-genesis in the BAT irrespective of mice fed with ND or HFD (Figure 2-4). Although CL-injection increased both UCP1and COX4 proteins in iWAT from mice given ND, it failed to induce both the protein expression in iWAT from HFD-induced obese mice, indicating that CL-dependent beige adipocyte induction in iWAT was impaired in diet-induced obese mice as well as in aged mice.

Thus, I next examined the number of PDGFRα-expressing progenitor using flow cytometry to determine its involvement in a possible mechanism of impaired β3-adrenergic agonist-mediated induction of beige adipocytes in obese mice. As shown in figure 2-5, the iWAT of HFD mice only contained a smaller number of PDGFRα-expressing progenitor cells ($7.55 \pm 0.42 \times 10^4$cells/depot) than that of ND mice ($1.49 \pm 0.12 \times 10^5$cells/depot), whereas there was no significant difference in the endothelial cell between ND and HFD mice. In addition, different from aged mice, M1 macrophage, but not M2 macrophage, in iWAT of HFD mice ($2.20 \pm 0.50 \times 10^4$ cells/depot), was also significantly higher than that in ND mice ($0.60 \pm 0.10 \times 10^4$ cells/depot) (Figure 2-5).

As M1 macrophages predominantly secrete inflammatory cytokines such as TNFα being involved in *Ucp1* expression in cultured adipocyte (10,11), effects of injections of TNFα for 3 consecutive days on cellular composition and *Ucp1* expression in iWAT were examined. TNFα-injections did not affect the numbers of PDGFRα-expressing progenitor, endothelial cell, and M1 and M2 macrophages in iWAT, compared with those of saline-injected mice (Figure 2-6 A). Moreover, TNFα-injection failed to affect CL-induced *Ucp1* mRNA expression (Figure 2-6 B). It is reported that WNT10 signaling is increased in WAT and may also be involved in the induction of beige adipocyte by influencing the number or differentiation of PDGFRα-expressing progenitor (76, 77). Thus, the expression of *Wnt10a* mRNA in iWAT was determined in our experimental conditions. *Wnt10a* expressions in BAT and iWAT from HFD mice were tended to be lower than the corresponding control of ND mice, at basal state without

CL-injection (Figure 2-7). In iWAT, there might be a tendency to increase of *Wnt10a* expression in response to CL-injection in mice given HFD, compared with mice fed with ND, although there was no statistical difference.

Next, the mRNA expression of each *Pdgf* isoform was determined. Among the *Pdgf* isoforms, *Pdgfb* and *Pdgfd* showed higher copy number of transcripts relative to *Pdgf*a and *Pdgfc* in both BAT and iWAT (Figure 2-8). In BAT, although mRNA expression of all the isoforms were not affected by HFD, mRNA expression of *Pdgfb* and *Pdgfc* were selectively increased by CL-injection. In iWAT, mRNA expression of *Pdgfd*, but not the others, tended to increase upon HFD feeding. Moreover, mRNA expression of *Pdgfb* in iWAT was significantly enhanced by CL-injection in ND mice, but the enhancement was blunted in HFD mice.

Treatment of mice with a PDGFR inhibitor, imatinib mesylate, together with CL injection, did not influence the number of PDGFRα-expressing progenitor in iWAT (Figure 2-9 A). However, treatment with imatinib mesylate significantly decreased UCP1, but not COX4, protein expression (Figure 2-9B).

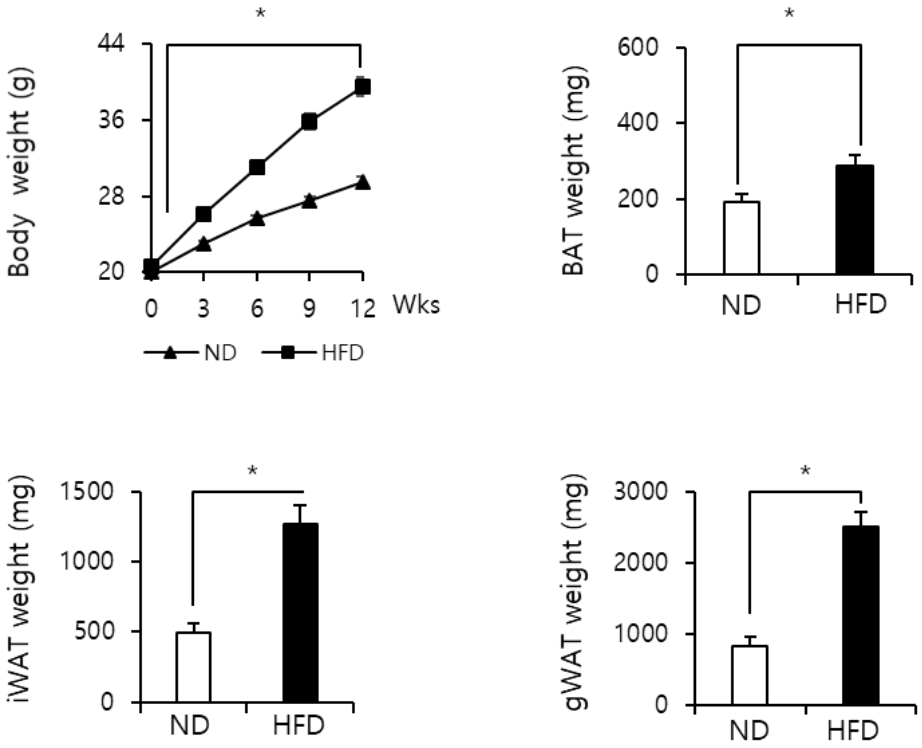


**Figure 2-1 Effects of normal or high-fat diet feeding on body weights and adipose tissue weight in mice**

Seven week-old male C57BL/6J mice were fed with normal diet (ND: 10kcal % fat) or high-fat diet (HFD: 45kcal % fat) for 3 months. Body weight was measured every three weeks. After 3-month of the feeding, interscapular brown adipose tissue (BAT) and inguinal (iWAT) and perigonadal (gWAT) white adipose tissues were excised and their weights were measured. Values are expressed as means ± SE for 6 mice. *p < 0.05 by Student's *t*-test.

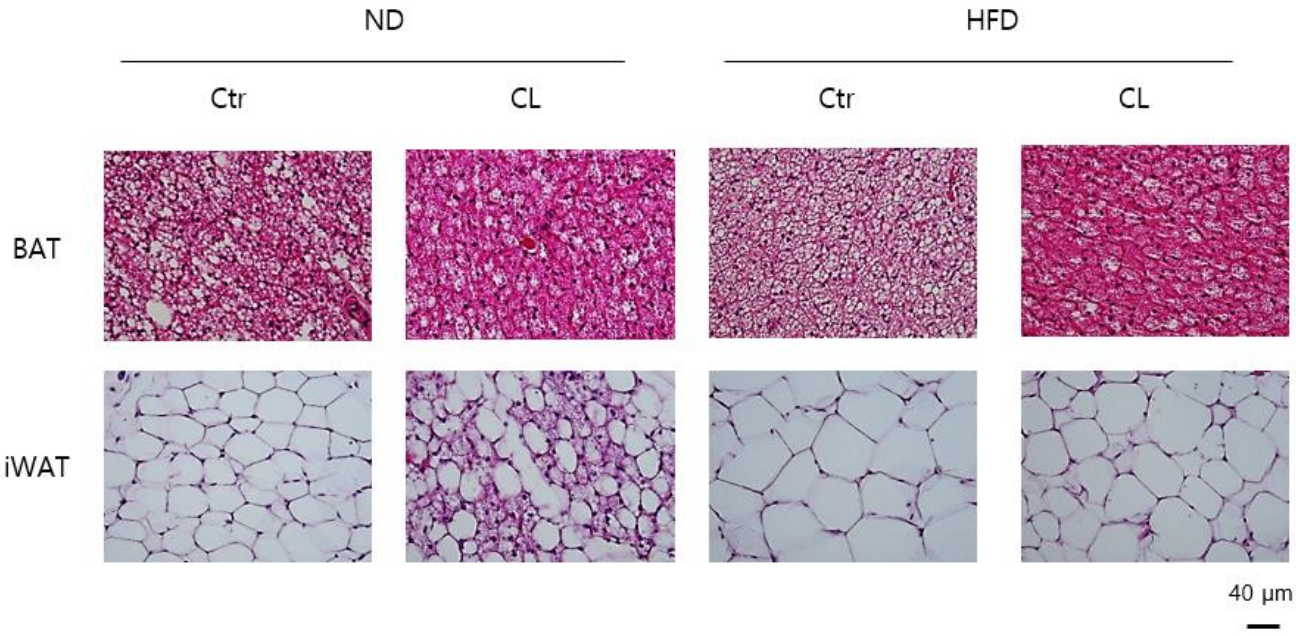


**Figure 2-2 Effect of β3-adrenergic agonist on morphological features of adipose tissue in mice fed with normal or high-fat diet**

Representative images of the sections stained with hematoxylin and eosin of BAT and iWAT of control or CL-injected ND and HFD mice.

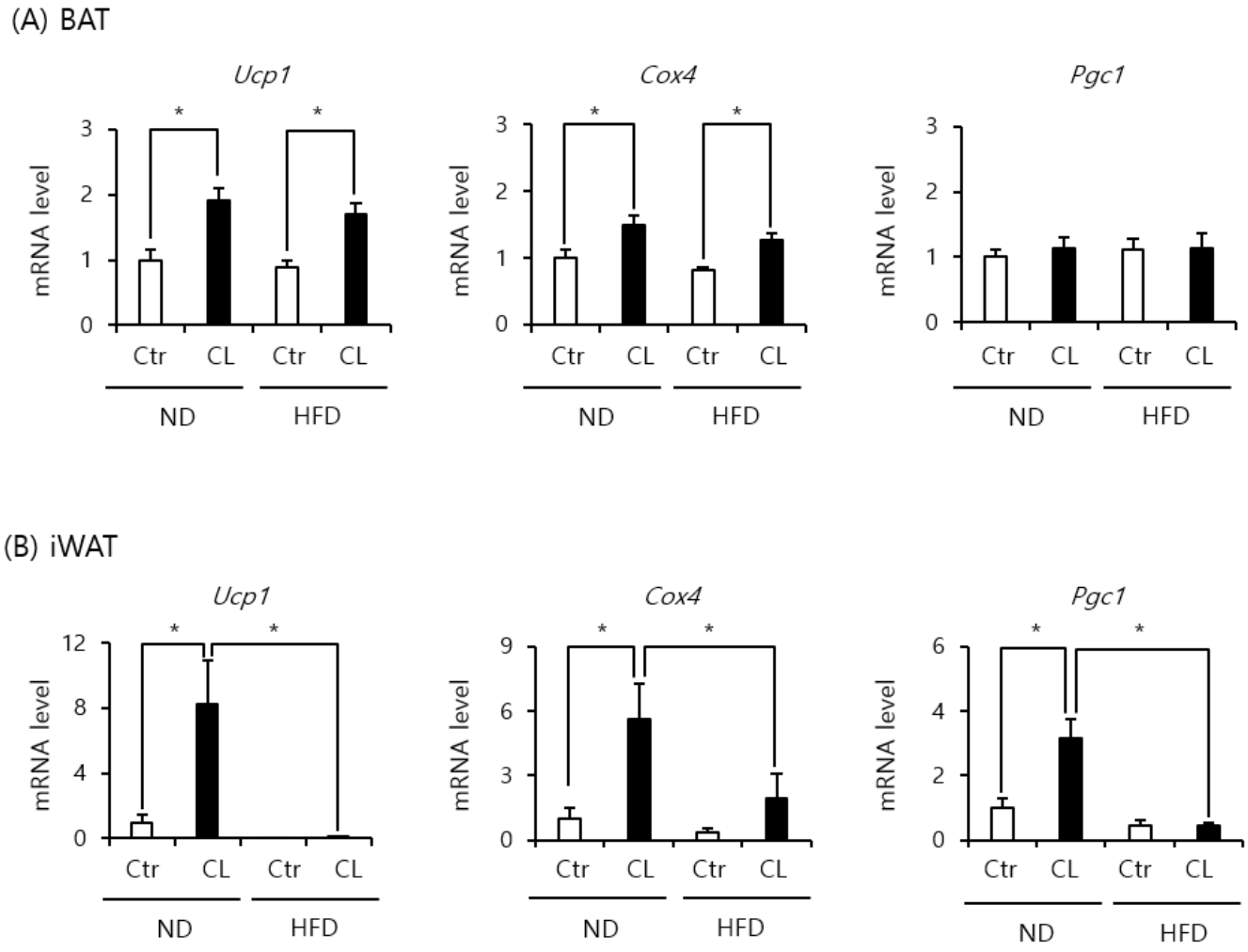


**Figure 2-3 Effect of β3-adrenergic agonist on mRNA expression of *Ucp1*, *Cox4* and *Pgc1* in the adipose tissues in mice fed with normal or high-fat diet**

Expression of the genes in BAT (A) and iWAT (B) of no-treatment control or CL-injected ND and HFD mice was analyzed by quantitative real-time PCR. Data normalized to *Actb* expression are expressed as relative value to control ND mice. Values are expressed as means ± SE for 4 mice. *p < 0.05 by ANOVA.

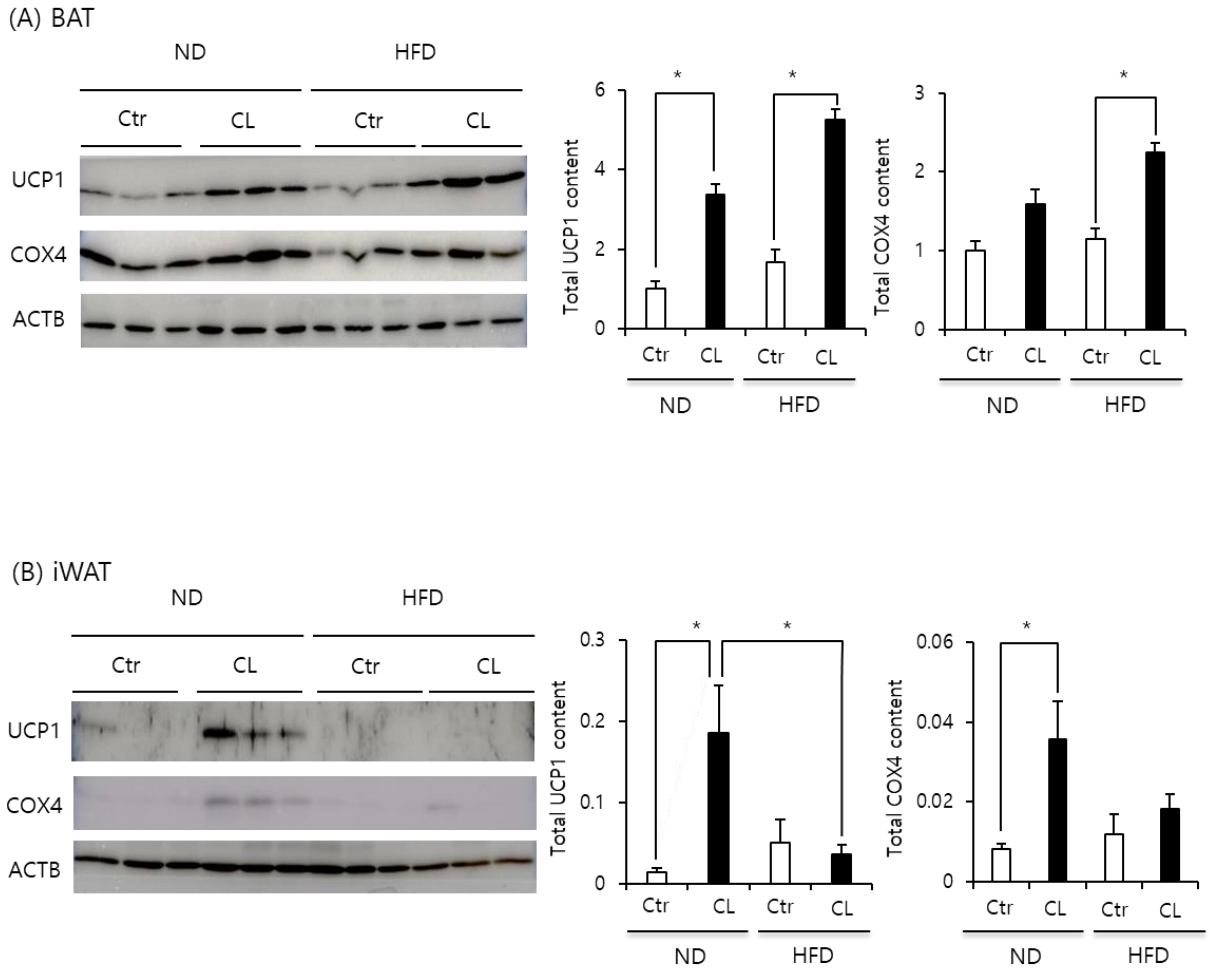


**Figure 2-4 Effect of β3-adrenergic agonist on protein expression in the adipose tissues in mice fed with normal or high-fat diet**

UCP1 and COX4 protein levels in BAT (A) and iWAT (B) of no-treatment control or CL-injected ND and HFD mice were analyzed by western blotting using 5 μg and 30 μg of total protein extracted from BAT and iWAT, respectively. ACTB is shown as a loading control. Total content of UCP1 and COX4 per depot was estimated by multiplying the protein amount detected by western blotting (arbitrary unit per μg protein) by the total protein extracted from whole depot (μg per depot), and expressed as relative value to the respective amounts in BAT of control ND mice. Values are expressed as means ± SE for 3-5 mice. *p < 0.05 by ANOVA.

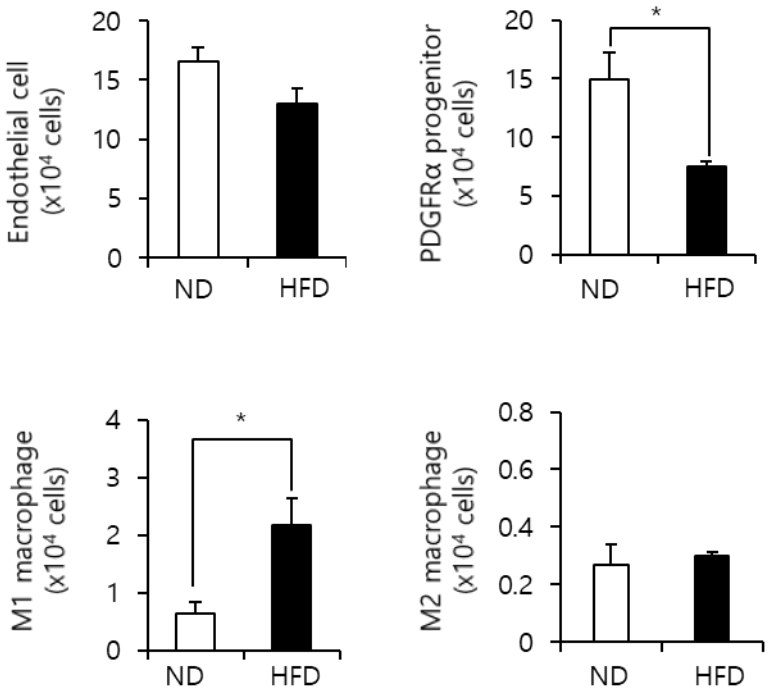


**Figure 2-5 The number of PDGFRα-expressing progenitor in the stromal vascular fraction of inguinal white adipose tissue in mice fed with normal or high-fat diet**

Cellular composition of the stromal vascular (SV) fraction isolated from iWAT was analyzed by flow cytometry. Comparison of endothelial cells ($CD31^+$), PDGFRα-expressing progenitors ($CD31^-$, $CD34^+$, $Sca1^+$, $PDGFR\alpha^+$), M1 macrophages ($F4/80^+$, $CD11c^+$, $CD206^-$), and M2 macrophages ($F4/80^+$, $CD11c^-$, $CD206^+$) between ND and HFD mice is shown. Values are expressed as means ± SE for 4 mice. *$p < 0.05$ by Student's *t*-test.

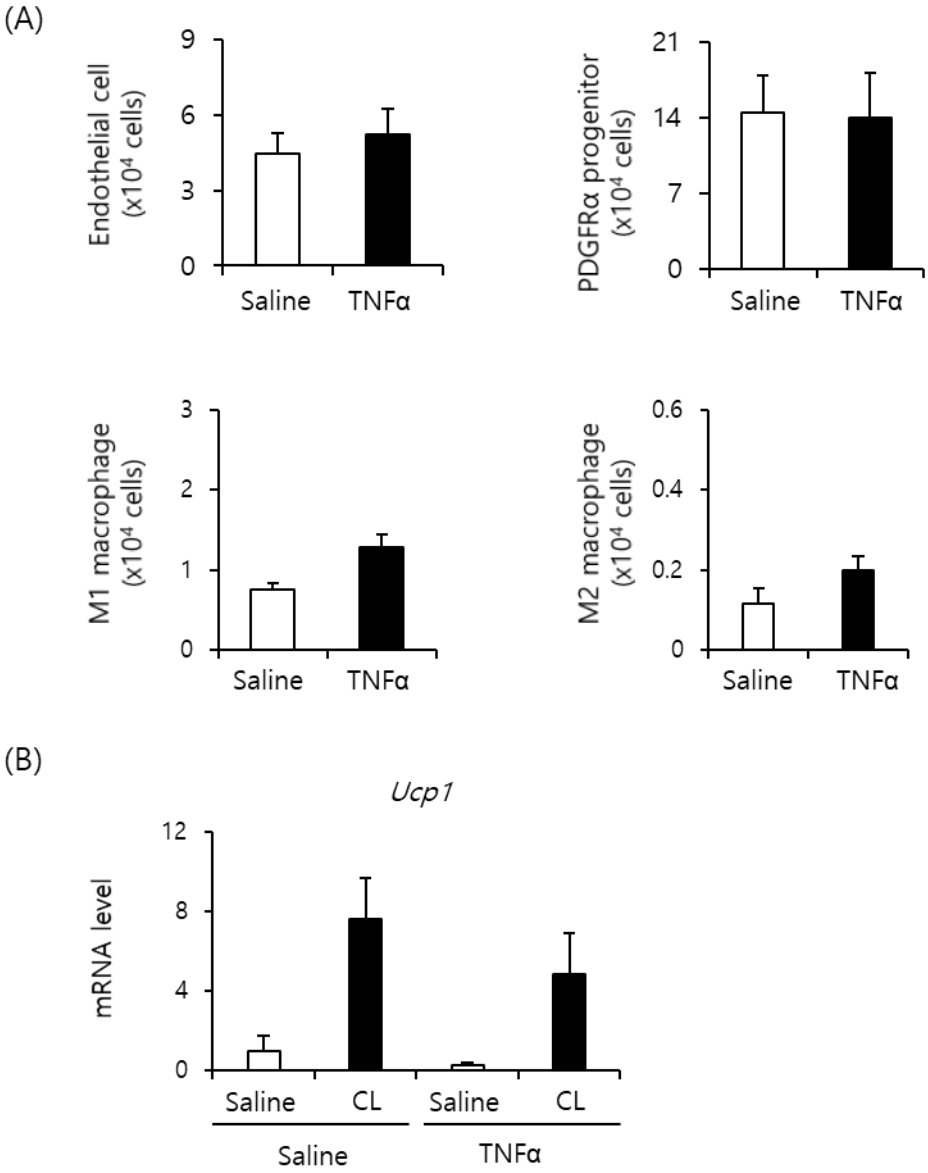


**Figure 2-6 Effect of TNF $\alpha$ on the number of PDGFR $\alpha$-expressing progenitor and β3-adrenergic agonist-induced *Ucp1* expression in the inguinal white adipose tissue**

Seven week-old male C57BL/6J mice were intraperitoneally injected with saline or TNF $\alpha$ (100 ug/kg, once a day) for 3 days. At the last injection, CL (0.1 mg/kg) or saline was also intraperitoneally injected. (A) Cellular composition of the stromal vascular (SV) fraction isolated from iWAT was analyzed by flow cytometry as described in the legend of Figure 2-5. (B) Expression of *Ucp1* in iWAT of each group of mice was analyzed by quantitative real-time PCR. Data normalized to *Actb* expression are expressed as relative value to the saline-injected mice. Values are expressed as means ± SE for 5 mice by Student's *t*-test (A) or ANOVA (B).

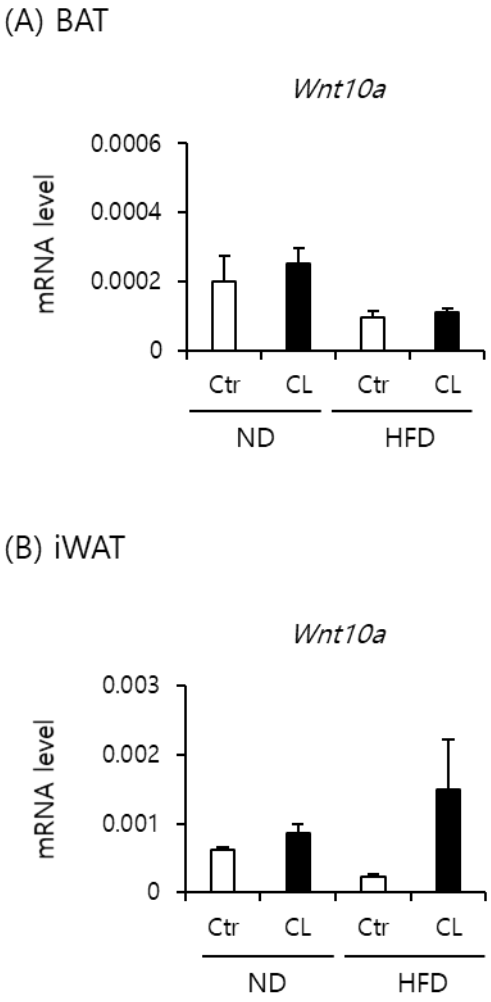


**Figure 2-7 Effect of β3-adrenergic agonist on mRNA expression of *Wnt10a* in the adipose tissue in mice fed with normal or high-fat diet**

Expression of the genes in BAT (A) and iWAT (B) of no-treatment control or CL-injected ND and HFD mice was analyzed by quantitative real-time PCR. Data normalized to *Actb* expression are expressed as means ± SE for 4 mice by ANOVA.

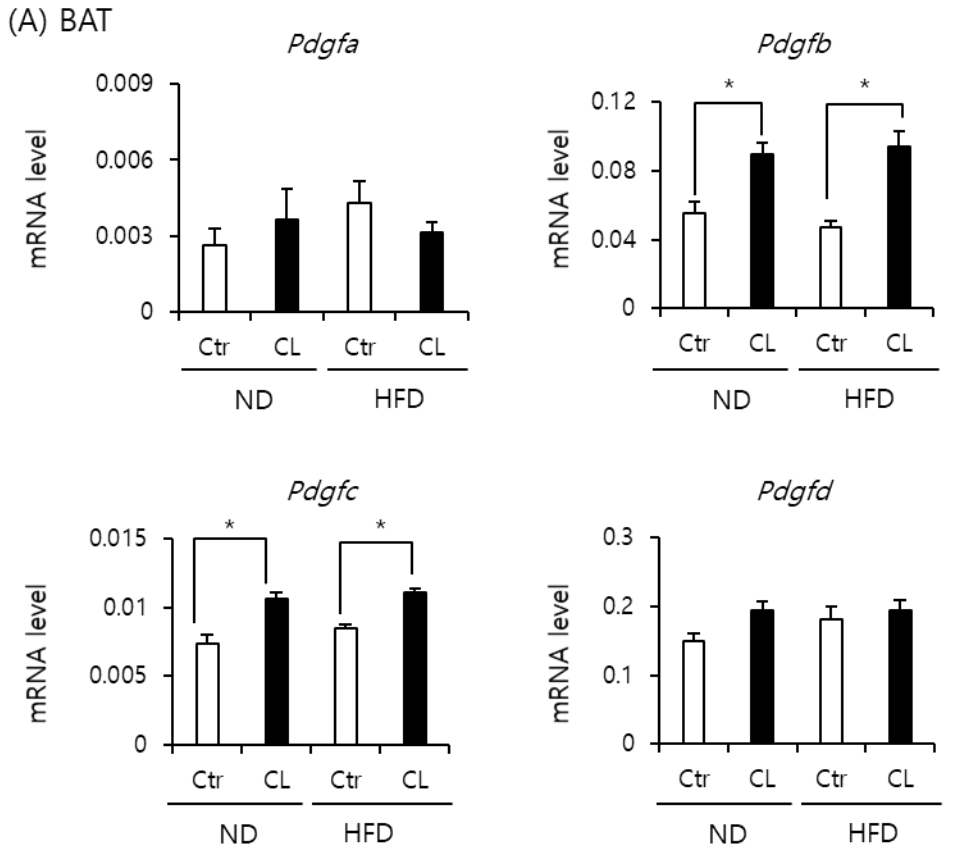
(A) BAT
Pdgfa
Pdgfb
Pdgfc
Pdgfd
mRNA level
0.009
0.006
0.003
0
0.12
0.08
0.04
0.015
0.01
0.005
0.3
0.2
0.1
*
Ctr
CL
ND
HFD

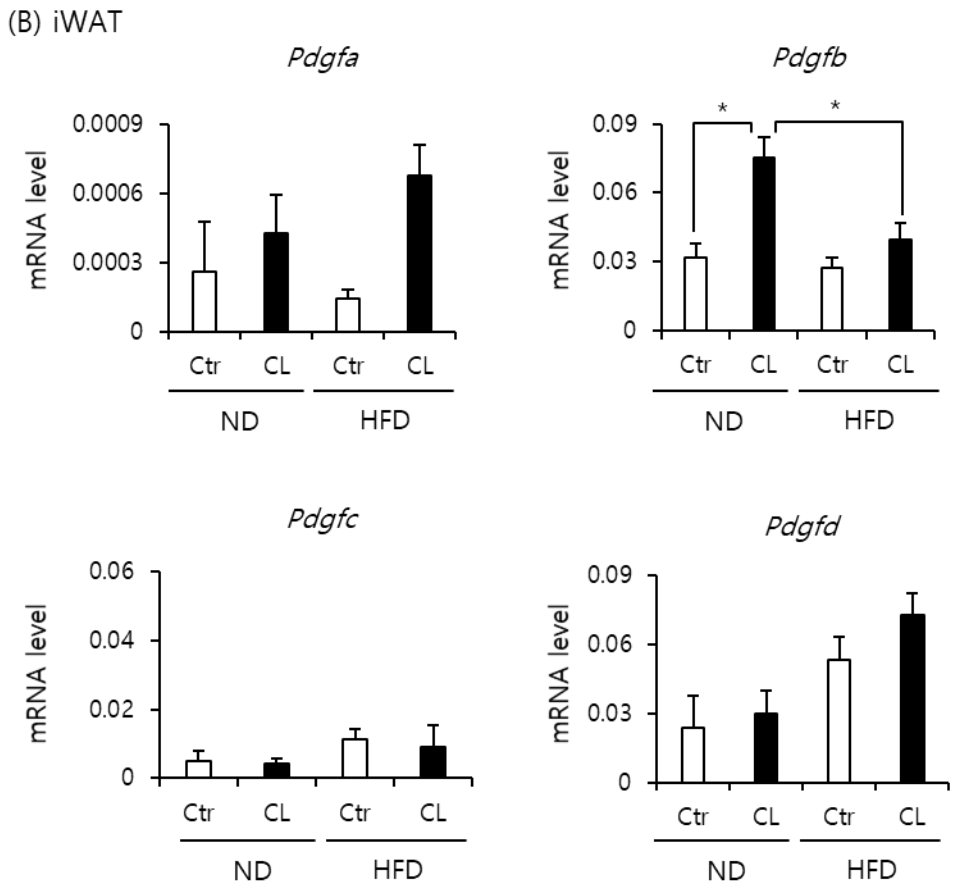
(B) iWAT
Pdgfa
Pdgfb
Pdgfc
Pdgfd
mRNA level
0.0009
0.0006
0.0003
0
0.09
0.06
0.03
0.04
0.02
*
Ctr
CL
ND
HFD

**Figure 2-8 Effect of $\beta$3-adrenergic agonist on mRNA expression of *Pdgf* isoforms in the adipose tissue in mice fed with normal or high-fat diet**

Expression of the genes in BAT (A) and iWAT (B) of no-treatment control or CL-injected ND and HFD mice was analyzed by quantitative real-time PCR. Data normalized to *Actb* expression are expressed as means ± SE for 4 mice. *p < 0.05 by ANOVA.

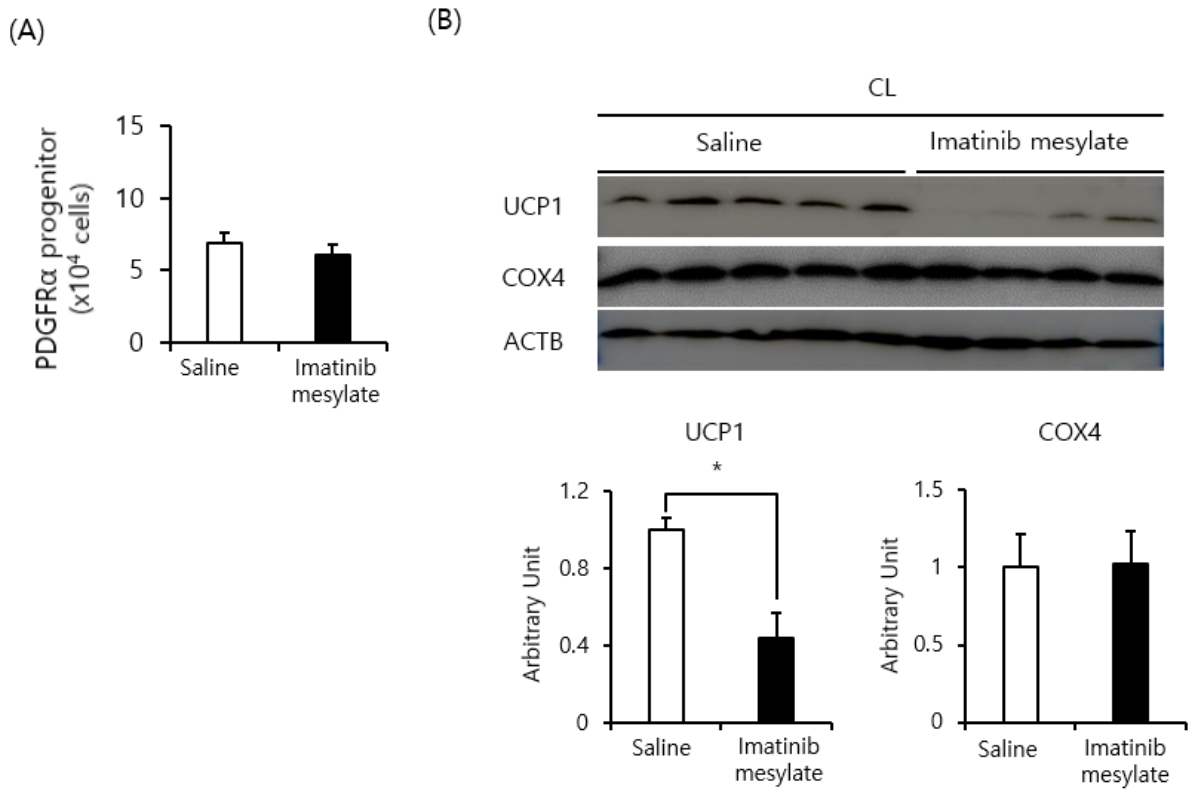


**Figure 2-9 Effect of PDGFR inhibitor on the number of PDGFRα-expressing progenitor and β3-adrenergic agonist-dependent UCP1 expression in the inguinal white adipose tissue**

Seven week-old male C57BL/6J mice were intraperitoneally injected with saline or imatinib mesylate (100 mg/kg, once a day) for 10 days. From the fourth day of PDGFR inhibitor injection, CL (0.1 mg/kg, once a day) was also intraperitoneally injected for 6 days. (A) Cellular composition of the stromal vascular (SV) fraction isolated from iWAT was analyzed by flow cytometry as described in the legend of Figure 2-5. Values are expressed as means ± SE for 6 mice. (B) UCP1 and COX4 protein levels in iWAT of saline- or imatinib mesylate-injected mice were analyzed by western blotting using 30 μg of total protein extracted from iWAT. ACTB is shown as a loading control. UCP1 and COX4 protein expression was estimated by western blotting (arbitrary unit), and expressed as relative value to saline-injected mice. Values are expressed as means ± SE for 4-5 mice. *$p < 0.05$ by Student's *t*-test.

**Discussion**

In chapter 2, the effect of diet-induced obesity on β3-adrenergic agonist-mediated beige adipocyte development in mice was examined. Mice fed with HFD for 14 weeks showed obese phenotypes such as hyperplasia of WAT, and almost complete abrogation of CL-induced mRNA and protein expression of UCP1 in iWAT where there was no apparent emergence of adipocytes containing multilocular lipid droplets. In contrast, expression of *Ucp1*and *Cox4* genes and their products were enhanced by CL-injection in BAT from HFD mice, whose morphological features were unchanged. These results indicate that CL-dependent beige adipocyte induction in iWAT was impaired in diet-induced obese mice, and coincide with those in aged mice as described in chapter 1. Since the decrease in the number of PDGFRα-expressing progenitors were observed in mice fed with HFD as well as in aged mice, compared with the corresponding control mice, it is likely that the reduction of the number of PDGFRα-expressing progenitor is one of the common mechanisms for the attenuation of beige adipocyte development both in aged and obese mice.

Unlike to aged mice, the number of M1 macrophage was increased in iWAT of mice given HFD, suggesting enhancement of infiltrated macrophage due to adipose tissue inflammation. Macrophage can be classified into M1- and M2-type, on the basis of its function. M1 macrophage is classically activated macrophage that secrets inflammatory cytokines such as TNFα, and infiltrates into WAT of obese animal (7, 44). As for the role of macrophages in beige adipocyte development, it was reported that the conditioned medium derived from lipopolysaccharide-activated macrophages suppressed the adrenergic stimulation-mediated UCP1 in C3H10T1/2 adipocytes, and the effect was canceled by the treatment with anti-TNFα antibody (71). In addition, TNFα treatment suppressed the promoter activity of the *Ucp1* gene *in vitro* (71). In this study, however, three consecutive daily TNFα injection failed to influence the number of PDGFRα-expressing progenitor and CL-dependent induction of *Ucp1* mRNA in

iWAT. It might be too short for TNF treatment to affect the number and phenotypes of PDGFRα-expressing progenitors in iWAT, when considered obesity developed period. More prolonged TNFα treatment *in vivo* might be necessary to clarify its role in beige adipocyte induction.

*Pdgfb* mRNA expression in iWAT of mice fed with ND increased in response to CL-injection, and the expression level was significantly lower in obese mice, while mRNA expression of the other three *Pdgf* isoforms were unaffected by the differences in diets given and in CL or saline-injection in iWAT. Moreover, *Pdgfb* mRNA expressed higher copy number of transcripts than *Pdgfa* and *Pdgfc* in iWAT, while *Pdgfd* expressed comparable levels with *Pdgfb*. It should be reminded that three homodimers, PDGF-AA, PDGF-BB and PDGF-CC, and one heterodimer, PDGF-AB are the ligands for PDGFRα, while PDGF-DD is for PDGFRβ (72, 73). Furthermore, injection of PDGFR inhibitor dramatically suppressed the CL-induced UCP1 protein expression in WAT without affecting the number of PDGFRα progenitors. In support of the above results, PDGF-BB enhances adipogenesis of orbital fibroblasts by enhancing the mRNA expression of peroxisome proliferator-activated receptor γ (PPARγ), a master regulator of adipogenesis (81) and a potent inducer of beige adipocyte through stabilization of PRD1-BF-1-RIZ1 homologous-domain-containing protein-16 (PRDM16) (44). Thus, although it is recently reported that PDGF-CC secreted from endothelial cell induces beige adipocyte in WAT (76), the present results strongly suggest that PDGF-B is the β-adrenergic agonist-regulatable dominant effector ligand for PDGFRα among the PDGF isoforms in iWAT to induce beige adipocyte differentiation, without influencing the progenitor recruitment, and that attenuated response of *Pdgfb* mRNA expression to adrenergic stimulation in obese state is one of the probable cause of the lowered beige adipocyte development.

It is well accepted that UCP1 contributes not only to cold-induced thermogenesis for the maintenance of body temperature but also to the diet-induced thermogenesis for the consumption of excess energy to maintain energy homeostasis, leading to preventing acute changes in body weight (82). Indeed, there is a report showing HFD feeding increases mRNA expression of *Ucp1* both in BAT and WAT (83). Also, diet-induced obese rats show elevated oxygen consumption, an index of energy expenditure, after NE-injection compared with control rat (84). In partly concert with the reports, although mRNA and protein levels of UCP1 in BAT without CL-injection were unchanged between ND and HFD groups, UCP1 protein along with COX4 protein increased by CL-injection in mice given HFD much more than those of ND in BAT. However, CL-induced UCP1 expression in iWAT was significantly suppressed by HFD feeding. Thus, the role of UCP1, especially that of beige adipocytes, in diet-induced thermogenesis is not clear in this study. Recently, various physiological roles other than thermogenesis have been proposed for beige adipocyte, including regulation of glucose homeostasis, blood triglyceride, and cholesterol (14, 18). It is possible that obesity-dependent suppression of beige adipocyte may exacerbate the symptom accompanied with hyperglycemia and hyperlipidemia in obesity. Further study is required to clarify the physiological role of beige adipocytes.

**Summary**

In chapter 2, I investigated the effect of high fat diet (HFD)-induced obesity on β3-adrenergic agonist-mediated beige adipocyte development in mice. Body weight and WAT weight in HFD mice were significantly higher compared to the mice fed with normal diet (ND). Treatment of ND mice with CL for 1 week induced mRNA and protein expression of UCP1 along with appearance of adipocytes containing multilocular lipid droplets in iWAT, whereas treatment of HFD mice by CL attenuated expression of not only *Ucp1* gene, but also *Cox4* and *Pgc1*, and distributed unilocular lipid droplet-containing adipocytes in iWAT. These results indicate that CL-dependent beige adipocyte induction in iWAT was impaired in diet-induced obese mice as well as in aged mice.

Flow cytometric analysis showed significant decrease in the number of PDGFRα-expressing progenitors for beige adipocytes and significant increase in the number of M1 macrophages in HFD mice compared with ND mice. However, treatment of mice with TNFα for three days failed to alter the number of PDGFRα-expressing progenitor cells and *Ucp1* gene expression in iWAT, suggesting TNFα produced by M1 macrophage, if present, is unlikely to be involved in the impairment. Next, the mRNA expression of four *Pdgf* isoforms were determined. In iWAT, only expression of *Pdgfb* mRNA was significantly enhanced by CL-injection in ND mice, but the enhancement was blunted in HFD mice. Furthermore, although treatment of mice with a PDGFR inhibitor, imatinib mesylate, together with CL injection, did not influence the number of PDGFRα-expressing progenitor in iWAT, it significantly decreased UCP1, but not COX4, protein expression. These results suggest that PDGF-B-activated PDGFRα-signaling pathway may contribute to beige adipocyte development possibly through the regulation of the differentiation, but not of the recruitment of beige adipocyte progenitors.

In conclusion, β3-adrenergic induction of beige adipocyte is attenuated with obesity in mice. The attenuation is at least in part due to the decreased number of PDGFRα-expressing

progenitors and the lowered PDGF-B-dependent signaling in obese mice.

Table2: Primer sequences for quantitative real time PCR used in the Chapter 2

| Gene name (gene symbol): NCBI Reference Sequence number, Product size<br>Forward primer sequence<br>Reverse primer sequence |
|---|
| *Actb*: NM_007393.5, 234 bp |
| For: 5’ - TCG TTA CCA CAG GCA TTG TGA T - 3’ |
| Rev: 5’ - TGC TCG AAG TCT AGA GCA AC - 3’ |
| *Ucp1*: NM_009463.3, 197 bp |
| For: 5’ - GTG AAG GTC AGA ATG CAA GC - 3’ |
| Rev: 5’ - AGG GCC CCC TTC ATG AGG TC - 3’ |
| *Cox4*: NM_009941.3, 252 bp |
| For: 5’ - TGA GCC TGA TTG GCA AGA GA - 3’ |
| Rev: 5’ - CGA AGC TCT CGT TAA ACT GG - 3’ |
| *Pgc1*: NM_008904.2, 214 bp |
| For: 5’ - GTG TGG AAC TCT CTG GAA CT - 3’ |
| Rev: 5’ - GCG TAC AAC TCA GAT TGC TC - 3’ |
| *Pdgfa*: NM_008808.3, 386 bp |
| For: 5’ - GAG GGA TGG TAC TGA ATT TCG C - 3’ |
| Rev: 5’ - TGC AAA CTG CAG GAA TGG CT - 3’ |
| *Pdgfb*: NM_011057.3, 94 bp |
| For: 5’ - ATG TGC CCT TCA GTC TGC TC - 3’ |
| Rev: 5’ - GAG ACA GGT CTC CTG CCC TA - 3’ |
| *Pdgfc*: NM_019971.2, 178 bp |
| For: 5’ - GCC CGA AGT TTC CTC ATA CA - 3’ |
| Rev: 5’ - ACA CTT CCA TCA CTG GGC TC - 3’ |

*Pdgfd*: NM_027924.2, 167 bp

For: 5’ - CGA GGG ACT GTG CAG TAG AAA - 3’

Rev: 5’ - TTG ATG GAT GCT CTC TGC GG - 3’

---

## CONCLUSION

Brown adipose tissue (BAT) is a tissue specialized for the thermogenic expenditure of energy and attracts a great attention as a therapeutic target of obesity and related metabolic diseases. In contrast to white adipose tissue (WAT) which is highly specialized for energy storage, BAT consumes lipid energy and generates heat. BAT thermogenesis is principally dependent on the activation of mitochondrial uncoupling protein 1 (UCP1), which uncouples oxidative phosphorylation to dissipate the electrochemical gradient as heat. Beige adipocyte is another type of UCP1-expressing adipocyte that appears in WAT after chronic sympathetic stimulation. Beige adipocytes have a similar thermogenic function to BAT at least *in vitro*, but their gene expression patterns and cell lineage are quite different from brown adipocytes. Interestingly, analyses of gene expression suggest that human BAT more closely resembles mouse beige adipocyte than brown adipocyte. Since PET-CT analyses reveal that presence of functional BAT in human adulthood is depend on age and adiposity, the aim of this study was to investigate the impact of aging or obesity on the beige adipocyte development in mice.

In chapter 1, I investigated the aging-related change of brown and beige adipocyte development in mice. Aged mice (20 months of age) had higher body weight than young mice (4 months of age), accompanied with an increase in peri-gonadal WAT weight and enlargement of adipocyte size. The results were coincident with the well-documented feature of the development of obesity in aged animal. Treatment with CL316,243 (CL), a selective ß3-AR agonist, increased UCP1 protein amounts in both BAT and inguinal WAT (iWAT), suggesting activation of brown and beige adipocytes. However, degree of beige adipocyte induction was impaired in aged mice, whereas brown adipocyte activation was comparable to young mice. The number of PDGFRα-expressing progenitor cells, which are able to differentiate into beige adipocytes, significantly decreased in iWAT of aged mice compared with that of young mice. These results revealed that inductivity of beige adipocytes in WAT reduces with aging in mice,

and that decreased number of progenitor cells is most likely involved in the impairment.

Aging is closely associated with increased adiposity by decreased metabolic rate, accompanied with increasing risk of obesity-related syndrome. Thus, I hypothesized that obesity is one of the mechanisms that accounts for the aging-related decline of beige adipocyte development.

In chapter 2, I investigated the obesity-related changes of beige adipocyte development in mice. Mice fed with high-fat diet (HFD) for 3 months gained significantly higher body weight and adiposity compared to mice fed with normal diet (ND). Treatment with CL for 1 week induced mRNA and protein expression of UCP1accompanied by the appearance of adipocytes containing multilocular lipid droplets in inguinal WAT in ND mice, whereas these changes were much attenuated in HFD mice. The number of PDGFRα-expressing progenitor cells was significantly reduced in HFD mice compared to ND mice, suggesting that the attenuation of beige adipocyte induction in obese mice is attributed to reduced number of progenitor cells.

To further characterize role of PDGFRα-expressing progenitor cells, I examined the mRNA expression of PDGF isoforms, ligands for PDGFRα, and found that *Pdgfb* mRNA expression was the highest among the isoforms and increased in response to CL-injection in ND mice. The *Pdgfb* mRNA expression after CL-injection was significantly lower in HFD mice compared ND mice. Moreover, the injection of PDGFR inhibitor suppressed CL-induced UCP1 expression in iWAT, although it showed no effect on the number of PDGFRα-expressing progenitor. These results suggest that PDGF-B-PDGFR pathway also plays role in beige adipocyte development by promoting differentiation, but not controlling progenitors number by proliferation.

In conclusion, I found that sympathetic stimulation-dependent beige adipocyte development in iWAT is impaired by aging and obesity in mice, while brown adipocyte development through β3-adrenergic receptor is unaltered. The impairment is most likely due

to obesity-dependent decreased number of PDGFRα-expressing progenitors and lowered *Pdgfb* mRNA expression.

In large mammal such as human classical BAT is lost in the childhood, and PET-CT-detectable beige-like brown cells work in the young adulthood, but vanish in the elder age who may develops obesity. Moreover, sympathetic stimulation is unlikely to activate both classical and PET-CT-detectable brown cells in the elder aged subject. Present results suggest that PDGFRα agonist may provide new therapeutic approach to combat obesity and related disease. However, more work is required to fully understand precious features of beige adipocyte.

**ACKNOWLEDGEMENTS**

First of all, I appreciate to Professor Kazuhiro KIMURA for giving me the opportunity studying here in Hokkaido university. Without his help and advices, I could have not started my study. Especially, I respect his educational philosophy which make student independent person who assumes the own responsibility. I also assure that he is a great leader who take care of student with deep trust and patience. Learned from him, I think that not only I have grown as an independent scientific researcher but also become mature man. Moreover, he tries to pay attention on the worry of the students and that was a huge support when I was in a slump. Above all, his unwavering presence was a great force to continue my research and the gratitude is beyond words.

I also thanks for Associate Professor Yuko OKAMATSU-OGURA. She taught strictly about scientific research and encouraged me to seek accurate scientific results. Throughout my degree, I have received from her invaluable scientific guidance, constructive criticism and generous supports. Especially, when I was disappointed with experimental failure, her warm and generous encouragement was unforgettable support which make me try and challenge again. Also, I deeply admire her dedicative efforts to brighten up the atmosphere of the laboratory in the midst of her busy schedule and it was a great help to me to adjust to the laboratory.

My great appreciation also goes to Assistant Professor Chitoku TODA. His wide knowledge on the latest scientific issues made me more challenging and impassioned. Also, his sharp criticism and debates helped me think more deeply about my research. Above all, I learned a lot from his humble attitude and characteristic which gave me deep impression.

I would like to offer my special thanks to my dissertation committee members Professor Osamu INANAMI and Associate Professor Ken-ichi OTSUGURO and for their excellent advices and critical reviewing of this thesis.

I am warmly grateful to all the present and former member at Laboratory of Biochemistry, Graduate School of Veterinary Medicine, Hokkaido University who directly or indirectly contributed to this project and help me to adjust to Japanese life. Especially, I thank for Ayumi, TSUBOTA, Takeshi YONESHIRO, Keigo FUKANO, Ryuji KAEDE and Shinya MATSUOKA, who taught me various experimental techniques. They used their precious time to teach me many experiments. Thanks for their advices, I was able to adapt quickly to the experiment. I also appreciate to Yuki MAKI, Machiko TERASHIMA and Nozomi TAMASHIRO for supporting administrative work. Thanks for their reassured support and kind advice, I could handle administrative work more easily and focus on research more during the course.

Most of all, I owe my family member who always encouraged and supported me. Their existence was huge reason that I could continue studying. Thank you so much for keeping a quiet and patience watch during the course. I know that it is the sweetest debt, I will ever have to pay.

## REFERENCES


1. Ghouse MS, Barwal SB, Wattamwar AS. A review on obesity. Health Science Journal Vol.10 No.4.13, 2016
2. Karageorgi S, Alsmadi O, Behbehani K. A review of adult obesity prevalence, trends, risk factors, and epidemiologic methods in Kuwait. J Obes 378650, 2013
3. World Health Organisation. Media centre-Obesity and overweight, 2017
4. World Health Organisation. Media centre-Obesity, 2017
5. Kahn SE, Hull RL, Utzshneider KM. Mechanisms linking obesity to insulin resistance and type 2 diabetes. Nature 14;444:840-846, 2006
6. Kelly T, Yang W, Chen CS, Reynolds K, He J. Global burden of obesity in 2005 and projections to 2030. Int J Obes (Lond) 32:1431-1437, 2008
7. Bai Y, Sun Q. Macrophage recruitment in obese adipose tissue. Obes Rev 16:127-136, 2015
8. Chen L, Chen R, Wang H, Liang F. Mechanisms linking inflammation to insulin resistance. Int J Endocrinol 508409, 2015
9. Basen-Engquist K, Chang M. Obesity and cancer risk: recent review and evidence. Curr Oncol Rep 13:71-76, 2011
10. Panee J. Monocyte chemoattractant protein 1 (MCP-1) in obesity and diabetes. Cytokine 60:1-12, 2012
11. Solinas G, Becattini B. JNK at the crossroad of obesity, insulin resistance, and cell stress response. Mol Metab 6:174-181, 2016
12. Hassan RH, Bourron O, Hajduch E. Defect of insulin signal in peripheral tissues: Important role of ceramide. World J Diabetes 5: 244–257, 2014
13. Muniyappa R, Sowers JR. Role of insulin resistance in endothelial dysfunction. Rev Endocr Metab Disord 14:5-12, 2013

14. Kajimura S, Saito M. A new era in brown adipose tissue biology: molecular control of brown fat development and energy homeostasis. Annu Rev Physiol 76:225-249, 2014

15. Inoue S, Egawa M, Satoh S, Saito M, Suzuki H, Kumahara Y, Abe M, Kumagai A, Goto Y, Shizume K. Clinical and basic aspects of an anorexiant, mazindol, as an antiobesity agent in Japan. Am J Clin Nutr 55:199S-202S, 1992

16. Cannon B, Nedergaard J. Brown adipose tissue: function and physiological significance. Physiol Rev 84:277-359, 2004

17. Harms M, Seale P. Brown and beige fat: development, function and therapeutic potential. Nature Medicine 19:1252-1263, 2013

18. Sidossis L, Kajimura S. Brown and beige fat in humans: thermogenic adipocytes that control energy and glucose homeostasis. J Clin Invest 125:478-486, 2015

19. Kajimura S, Spiegelman BM, Seale P. Brown and beige fat: physiological roles beyond heat generation. Cell Metab 22: 546–559, 2015

20. Ikeda K, Maretich P, Kajimura S. The common and distinct features of brown and beige adipocytes. Trends Endocrinol Metab 29:191-200, 2018

21. Himms-Hagen J, Cui J, Danforth E Jr, Taatjes DJ, Lang SS, Waters BL, Claus TH. Effect of CL-316,243, a thermogenic beta 3-agonist, on energy balance and brown and white adipose tissues in rats. Am J Physiol 266:R1371-R1382, 1994

22. Nagase I, Sasaki N, Tsukazaki K, Yoshida T, Morimatsu M, Saito M. Hyperplasia of brown adipose tissue after chronic stimulation of beta 3-adrenergic receptor in rats. Jpn J Vet Res 42:137-145, 1994

23. Okamatsu-Ogura Y, Tsubota A, Ohyama K, Nogusa Y, Saito M, Kimura K. Capsinoids suppress diet-induced obesity through uncoupling protein 1-dependent mechanism in mice. J Funct Foods 19 1-9, 2015

24. Feldmann HM, Golozoubova V, Cannon B, Nedergaard J. UCP1 ablation induces obesity and abolishes diet-induced thermogenesis in mice exempt from thermal stress by living at thermoneutrality. Cell Metab 9:203-209, 2009

25. Van der Lans AA, Hoeks J, Brans B, Vijgen GH, Visser MG, Vosselman MJ, Hansen J, Jörgensen JA, Wu J, Mottaghy FM, Schrauwen P, van Marken Lichtenbelt WD. Cold acclimation recruits human brown fat and increases nonshivering thermogenesis. J Clin Invest 123:3395-3403, 2013

26. Trayhurn P. Recruiting Brown adipose tissue in human obesity. Diabetes 65:1158-1160, 2016

27. Okamatsu-Ogura Y, Fukano K, Tsubota A, Uozumi A, Terao A, Kimura K, Saito M. Thermogenic ability of uncoupling protein 1 in beige adipocytes in mice. PLoS One 8:e84229, 2013

28. Shabalina IG, Petrovic N, de Jong JM, Kalinovich AV, Cannon B, Nedergaard J. UCP-1 in brite/beige adipose tissue mitochondria is functionally thermogenic. Cell Rep 5:1196-1203, 2013

29. Petrovic N, Walden TB, Shabalina IG, Timmons JA, Cannon B, Nedergaard J. Chronic peroxisome proliferator-activated receptor gamma (PPARgamma) activation of epididymally derived white adipocyte cultures reveals a population of thermogenically competent, UCP-1-containing adipocytes molecularly distinct from classic brown adipocytes. J Biol Chem 285:7153-7164, 2010

30. Wu J, Boström P, Sparks LM, Ye L, Choi JH, Giang AH, Khandekar M, Virtanen KA, Nuutila P, Schaart G, Huang K, Tu H, van Marken Lichtenbelt WD, Hoeks J, Enerbäck S, Schrauwen P, Spiegelman BM. Beige adipocytes are a distinct type of thermogenic fat cell in mouse and human. Cell 150:366-76, 2012

31. Walden TB, Hansen IR, Timmons JA, Cannon B, Nedergaard J. Recruited versus nonrecruited molecular signatures of brown, ″brite,″ and white adipose tissues. Am J Physiol Endocr Metab 302:E19–E31, 2012

32. Sharp LZ, Shinoda K, Ohno H, Scheel DW, Tomoda E, Ruiz L, Hu H, Wang L, Pavlova Z, Gilsanz V, Kajimura S. Human BAT possesses molecular signatures that resemble beige/brite cells. PLoS ONE 7:e49452, 2012

33. Ghorbani M, Himms-Hagen J. Appearance of brown adipocytes in white adipose tissue during CL 316,243-induced reversal of obesity and diabetes in Zucker fa/fa rats. Int J Obes Relat Metab Disord 21:465-475, 1997

34. Cousin B, Cinti S, Morroni M, Raimbault S, Ricquier D, Pénicaud L, Casteilla L. Occurrence of brown adipocytes in rat white adipose tissue: molecular and morphological characterization. J Cell Sci 103: 931-942, 1992

35. Contreras GA, Lee YH, Mottillo EP, Granneman JG. Inducible brown adipocytes in subcutaneous inguinal white fat: the role of continuous sympathetic stimulation. Am J Physiol Endocrinol Metab 307:793-799, 2014

36. Jimenez M, Barbatelli G, Allevi R, Cinti S, Seydoux J, Giacobino JP, Muzzin P, Preitner F. Beta3-adrenoreceptor knockout in C57BL/6J mice depresses the occurrence of brown adipocyte in white fat. Eur J Biochem 270:699-705, 2003

37. Villarroya F, Cereijo R, Villarroya J, Gavaldà-Navarro A, Giralt M. Toward an understanding of how immune cells control brown and beige adipobiology. Cell Metab 27:954-961, 2018

38. Huang Z, Zhong L, Lee JTH, Zhang J, Wu D, Geng L, Wang Y, Wong CM, Xu A. The FGF21-CCL11 axis mediates beiging of white adipose tissues by coupling sympathetic nervous system to type 2 immunity. Cell Metab 26:493-508, 2017

39. Liu D, Ceddia RP, Collins S. Cardiac natriuretic peptides promote adipose 'browning' through mTOR complex-1. Mol Metab 9:192-198, 2018

40. Yoneshiro T, Aita S, Matsushita M, Okamatsu-Ogura Y, Kameya T, Kawai Y, Miyagawa M, Tsujisaki M, Saito M. Age-related decrease in cold-activated brown adipose tissue and accumulation of body fat in healthy humans. Obesity (Silver Spring) 19:1755-1760, 2011

41. Leitner BP, Huang S, Brychta RJ, Duckworth CJ, Baskin AS, McGehee S, Tal I, Dieckmann W, Gupta G, Kolodny GM, Pacak K, Herscovitch P, Cypess AM, Chen KY. Mapping of human brown adipose tissue in lean and obese young men. Proc Natl Acad Sci U S A 114:8649-8654, 2017

42. Nguyen KD, Qiu Y, Cui X, Goh YP, Mwangi J, David T, Mukundan L, Brombacher F, Locksley RM, Chawla A. Alternatively activated macrophage produce catecholamines to sustain adaptive thermogenesis. Nature 480:104-108, 2011

43. Hui X, Gu P, Zhang J, Nie T, Pan Y, Wu D, Feng T, Zhong C, Wang Y, Lam KS, Xu A. Adiponectin enhanced cold-induced browning of subcutaneous adipose tissue via promoting M2 macrophage proliferation. Cell Metab 22:279-290, 2015

44. Sakamoto T, Nitta T, Maruno K, Yeh YS, Kuwata H, Tomita K, Goto T, Takahashi N, Kawada T. Macrophage infiltration into obese adipose tissues suppresses the induction of UCP-1 level in mice. Am J Physiol Endocrinol Metab 310:676-687, 2016

45. Barbatelli G, Murano I, Madsen L, Hao Q, Jimenez M, Kristiansen K, Giacobino JP, De Matteis R, Cinti S. The emergence of cold-induced brown adipocytes in mouse white fat depots is determined predominantly by white to brown adipocyte transdifferentiation. Am J Physiol Endocrinol Metab 298:E1244-E1253, 2010

46. Ohno H, Shinoda K, Spiegelman BM, Kajimura S. PPARγ agonists induce a white-to-brown fat conversion through stabilization of PRDM16 protein. Cell Metab 15:395–404, 2012

47. Altshuler-Keylin S, Shinoda K, Hasegawa Y, Ikeda K, Hong H, Kang Q, Yang Y, Perera RM, Debnath J, Kajimura S. Beige adipocyte maintenance is regulated by autophagy-induced mitochondrial clearance. Cell Metab 24:402-419, 2016

48. Lu X, Altshuler-Keylin S, Wang Q, Chen Y, Henrique Sponton C, Ikeda K, Maretich P, Yoneshiro T, Kajimura S. Mitophagy controls beige adipocyte maintenance through a Parkin-dependent and UCP1-independent mechanism. Sci Signal 11: eaap8526, 2018

49. Wang QA, Tao C, Gupta RK, Scherer PE. Tracking adipogenesis during white adipose tissue development, expansion and regeneration. Nat Med 19:1338-1344, 2013

50. Lee YH, Petkova AP, Mottillo EP, Granneman JG. In vivo identification of bipotential adipocyte progenitors recruited by b3-adrenoceptor activation and high fat feeding. Cell Metab 15:480-491, 2012

51. Sikder D, Sellayah D. Orexin restores aging-related brown adipose tissue dysfunction in male mice. Endocrinology 155:485-501, 2014

52. Florez-Duquet M, Horwitz BA, McDonald RB. Cellular proliferation and UCP content in brown adipose tissue of cold-exposed aging Fischer 344 rats. Am J Physiol 274:R196-R203, 1998

53. Schulz TJ, Graja A. Mechanisms of aging-related impairment of brown adipocyte development and function. Gerontology 61:211-217, 2015

54. Florez-Duquet M, Horwitz BA, McDonald RB. Cellular proliferation and UCP content in brown adipose tissue of cold-exposed aging Fischer 344 rats. Am J Physiol 274:R196-R203, 1998

55. Cypess AM, Lehman S, Williams G, Tal I, Rodman D, Goldfine AB, Kuo FC, Palmer EL, Tseng YH, Doria A, Kolodny GM, Kahn CR. Identification and importance of brown adipose tissue in adult humans. N Engl J Med 360:1509-1517, 2009

56. Healton JM. The distribution of brown adipose tissue in the human. J Anat 112: 35–39, 1972

57. Pfannenberg C, Werner MK, Ripkens S, Stef I, Deckert A, Schmadl M, Reimold M, Häring HU, Claussen CD, Stefan N. Impact of age on the relationships of brown adipose tissue with sex and adiposity in humans. Diabetes 59:1789-1793, 2010

58. Rogers NH, Landa A, Park S, Smith RG. Aging leads to a programmed loss of brown adipocytes in murine subcutaneous white adipose tissue. Aging Cell 11: 1074-1083, 2012

59. Wellen KE, Hotamisligil GS. Obesity-induced inflammatory changes in adipose tissue. J Clin Invest 112:1785-1788, 2003

60. Nedergaard J, Cannon B. UCP-1 mRNA does not produce heat. Biochim Biophys Acta 1831:943-949, 2013

61. Kirkland JL, Tchkonia T, Pirtskhalava T, Han J, Karagiannides I. Adipogenesis and aging: does aging make fat go MAD?. Exp Gerontol 37:757-767, 2002

62. Lumeng CN, Liu J, Geletka L, Delaney C, Delproposto J, Desai A, Oatmen K, Martinez-Santibanez G, Julius A, Garg S, Yung RL. Aging is associated with increase in T cells and inflammatory macrophage in visceral adipose tissue. J Immunol 187:6208-6216, 2011

63. Bapat SP, Myoung Suh J, Fang S, Liu S, Zhang Y, Cheng A, Zhou C, Liang Y, LeBlanc M, Liddle C, Atkins AR, Yu RT, Downes M, Evans RM, Zheng Y. Depletion of fat-resident Treg cells prevents age-associated insulin resistance. Nature 528:137-141, 2015

64. Goto T, Naknukool S, Yoshitake R, Hanafusa Y, Tokiwa S, Li Y, Sakamoto T, Nitta T, Kim M, Takahashi N, Yu R, Daiyasu H, Seno S, Matsuda H, Kawada T. Proinflammatory cytokine interleukin-1b suppresses cold-induced thermogenesis in adipocyte. Cytokine 77:101-114, 2016

65. Wu D, Ren Z, Pae M, Guo W, Cui X, Merrill AH, Meydani SN. Aging up-regulates expression of inflammatory mediators in mouse adipose tissue. Immunol 179:4829-4839, 2007

66. Berry DC, Jiang Y, Arpke RW, Close EL, Uchida A, Reading D, Berglund ED, Kyba M, Graff JM. Cellular aging contributes to failure of cold-induced beige adipocyte formation in old mice and humans. Cell Metab 25:166-181, 2017

67. Fu W, Liu Y, Sun C, Yin H. Transient p53 inhibition sensitizes aged white adipose tissue for beige adipocyte recruitment by blocking mitophagy. FASEB J 27:fj201800577R, 2018

68. Jura M, Kozak LP. Obesity and related consequences to ageing. Age (Dordr) 38:23, 2016

69. Sam S, Mazzone T. Adipose tissue changes in obesity and the impact on metabolic function. Transl Res 164:284-292, 2014

70. Martins FF, Bargut TCL, Aguila MB, Mandarim-de-Lacerda CA. Thermogenesis, fatty acid synthesis with oxidation, and inflammation in the brown adipose tissue of ob/ob (−/−) mice. Ann Anat 210:44-51, 2017

71. Sakamoto T, Takahashi N, Sawaragi Y, Naknukool S, Yu R, Goto T, Kawada. Inflammation induced by RAW macrophages suppresses UCP1 mRNA induction via ERK activation in 10T1/2 adipocytes. Am J Physiol Cell Physiol 304:C729-C738, 2013

72. Dani C, Pfeifer A. The complexity of PDGFR signaling: regulation of adipose progenitor maintenance and adipocyte-myofibroblast transition. Stem Cell Investig 4:28, 2017

73. Chen PH, Chen X, He X. Platelet-derived growth factors and their receptors: structural and functional perspectives. Biochim Biophys Acta 1834:2176-2186, 2013

74. Choudhury GG, Marra F, Kiyomoto H, Abboud HE. PDGF stimulates tyrosine phosphorylation of JAK 1 protein tyrosine kinase in human mesangial cells. Kidney Int 49:19-25, 1996

75. Seki T, Hosaka K, Lim S, Fischer C, Honek J, Yang Y, Andersson P, Nakamura M, Näslund E, Ylä-Herttuala S, Sun M, Iwamoto H, Li X, Liu Y, Samani NJ, Cao Y. Endothelial PDGF-CC regulates angiogenesis-dependent thermogenesis in beige fat. Nat Commun 7:12152, 2016

76. Cohen ED, Ihida-Stansbury K, Lu MM, Panettieri RA, Jones PL, Morrisey EE. Wnt signaling regulates smooth muscle precursor development in the mouse lung via a tenascin C/PDGFR pathway. J Clin Invest 119:2538-2549, 2009

77. Kang S, Bajnok L, Longo KA, Petersen RK, Hansen JB, Kristiansen K, MacDougald OA. Effects of Wnt signaling on brown adipocyte differentiation and metabolism mediated by PGC-1alpha. Mol Cell Biol 25:1272-1282, 2005

78. Karczewska-Kupczewska M, Stefanowicz M, Matulewicz N, Nikołajuk A, Strączkowski M. Wnt signaling genes in adipose tissue and skeletal muscle of humans with different Degrees of Insulin Sensitivity. J Clin Endocrinol Metab 101:3079-3087, 2016

79. Wada N, Hashinaga T, Otabe S, Yuan X, Kurita Y, Kakino S, Ohoki T, Nakayama H, Fukutani T, Tajiri Y, Yamada K. Selective modulation of Wnt ligands and their receptors in adipose tissue by chronic hyperadiponectinemia. PLoS One 8:e67712, 2013

80. Lo KA, Ng PY, Kabiri Z, Virshup D, Sun L. Wnt inhibition enhances browning of mouse primary white adipocytes. Adipocyte 5:224-231, 2016

81. Virakul S, Dalm VA, Paridaens D, van den Bosch WA, Mulder MT, Hirankarn N, van Hagen PM, Dik WA. Platelet-derived growth factor-BB enhances adipogenesis in orbital fibroblasts. Invest Ophthalmol Vis Sci 56:5457-5464, 2015

82. Fromme T, Klingenspor M. Uncoupling protein 1 expression and high-fat diets. Am J Physiol Regul Integr Comp Physiol 300:R1-R8, 2011

83. García-Ruiz E, Reynés B, Díaz-Rúa R, Ceresi E, Oliver P, Palou A. The intake of high-fat diets induces the acquisition of brown adipocyte gene expression features in white adipose tissue. Int J Obes (Lond) 39:1619-1629, 2015

84. Rothwell NJ, Stock MJ, Warwick BP. Energy balance and brown fat activity in rats fed cafeteria diets or high-fat, semisynthetic diets at several levels of intake. Metabolism 34:474-480, 1985

**JAPANESE SUMMARY**

# Study on development of brown and beige adipocytes in mice: effect of age and diet-induced obesity

(マウスにおける褐色およびベージュ脂肪細胞の誘導・発達に関する研究：加齢および食餌誘導性肥満の影響)

Woongchul SHIN

シン　ウンチョル

褐色脂肪組織（BAT）はエネルギーを消費して熱を生産する特殊な脂肪組織であり、エネルギー消費の側面からの肥満対策のターゲットとして関心をあつめている。褐色脂肪細胞は多房性脂肪滴を含み、ミトコンドリア内膜に発現する脱共役 タンパク質（Uncoupling protein 1; UCP1）が脂肪エネルギーを消費して熱を産生する。褐色脂肪細胞とは対照的に、白色脂肪組織（WAT）中の白色脂肪細胞は単房性脂肪滴を含み、 余剰なエネルギーを中性脂肪として貯蔵する。ベージュ脂肪細胞は、アドレナリン性刺激によって WAT 中に出現し、UCP1 発現する脂肪細胞である。形態や熱産生機能は褐色脂肪細胞と似ているが、遺伝子発現や発生過程での起源細胞が異なる。興味深いことに、ヒト褐色脂肪組織の遺伝子発現パターンは、マウスの褐色脂肪細胞よりベージュ脂肪細胞に近いことが明らかになっている。したがって、ベージュ脂肪細胞の誘導メカニズムを明らかにすることは、肥満対策の新たな治療戦略の確立に役立つと考えられる。本研究では、加齢や肥満がベージュ脂肪細胞の誘導性にどのような影響を与えるかを明らかにすることを目的とした。

第 1 章では老化に伴うベージュの脂肪細胞誘導性の変化を調べた。20 ヶ月齢の老齢マウスでは、4 ヶ月齢の成マウスに比べて体重および白色脂肪組織重量が有意に大きかった。白色脂肪細胞サイズが肥大化しており、いわゆる加齢性肥満を生じていると考えられた。ß3 アドレナリン受容体アゴニストである CL316,243（CL）を 1 週間投与すると、BAT と WAT のいずれにおいても UCP1 タンパク質の発現が増加し、褐色およびベージュ脂肪細胞が活性化していると考えられた。しかし、褐色脂肪細胞の活性化には成マウスと老齢マウスで違いはなかったが、ベージュ脂肪細胞の誘導性は成マウスに比べて老齢マウスで有意に抑制された。老化によるベージュ脂肪細胞誘導性低下のメカニズムを明らかにするために、ベージュ脂肪細胞に分化することが報告されてる PDGFRαを発現する前駆細胞（PDGFRα細胞）の数を調べると、成マウスに比較して、老齢マウスの iWAT において PDGFRα細胞の数が有意に低かった。以上の結果から、アドレナリン性刺激によるベージュ脂肪細胞の誘導性は、老化に伴い低下することが明らかになった。そのメカニズムとして、前駆細胞の数の減少がかかわることが示唆された。

老化に伴う代謝量の低下は内臓脂肪の蓄積を引き起こし、肥満症の発症リスクを増加させる。実際、本研究においても老化マウスは体脂肪量の有意な増加を示した。そこで、老化に伴うベージュ脂肪細胞誘導性の低下に肥満に伴う脂肪組織の肥大化が影響している可能性を考えた。

第 2 章では、肥満マウスにおけるベージュ脂肪細胞誘導性の変化を調べた。マウスに高脂肪食（HFD）または通常食（ND）を 14 週間与えると、HFD 群では体重と WAT 重量が ND 群に比べて有意に大きくなった。CL を 1 週間投与すると、ND 群の WAT では UCP1 の mRNA およびタンパク質発現が増加し、多房性脂肪滴を含む脂

肪細胞が出現したが、HFD 群ではこれらの反応が減弱していた。また、WAT における PDGFRα細胞の数は ND 群に比べて HFD 群で有意に少なく、肥満によるベージュ脂肪細胞誘導性の低下の一因である可能性が考えられた。

PDGFRα細胞の数の制御機構を明らかにするために、PDGFRαのリガンドである PDGF の遺伝子発現を調べた。PDGF の 4 つのアイソフォームのうち、WAT では PDGF−B が最も高い発現量を示し、 ND 群において CL 投与により増加する傾向があった。一方、HFD 群においては変化が認められず、CL 投与後の発現量は ND 群に比べて有意に低かった。さらに、PDGFR 阻害剤の投与は、PDGFRα細胞の数には影響を与えなったが、CL 投与により誘導される UCP1 発現を抑制した。これらの結果から、PDGF-B-PDGFRα経路の活性化は、前駆細胞の数ではなく分化を促進することで、ベージュ脂肪細胞を誘導する可能性が考えられた。

以上の研究により、マウスにおいて老化と肥満はベージュ脂肪細胞誘導性を低下させることが明らかになった。そのメカニズムとして、PDGFRαを発現するベージュ前駆細胞の数と PDGF−B 依存的シグナル経路の活性の低下が要因である可能性が考えられた。本研究の結果は、適切な数のベージュ前駆細胞と分化誘導経路を維持することがベージュ脂肪細胞誘導性の維持につながることを示唆しており、肥満と肥満に関連した病態の新たな治療戦略の確立に貢献することが期待される。